Rearrangement of Iridabenzvalenes to Iridabenzenes and/or η^5-Cyclopentadienyliridium(I) Complexes: Experimental and Computational Analysis of the Influence of Silyl Ring Substituents and Phosphine Ligands§

He-Ping Wu,† Daniel H. Ess,‡,# Seren Lanza,† Timothy J. R. Weakley,† K. N. Houk,# Kim K. Baldridge,*,‡ and Michael M. Haley*,†

Department of Chemistry, University of Oregon, Eugene, Oregon 97403-1253, Institute of Organic Chemistry, University of Zürich, Winterthurerstrasse 190, CH-8057 Zürich, Switzerland, and Department of Chemistry and Biochemistry, University of California, Los Angeles, California 90095

Received April 5, 2007

Lithium−halogen exchange of either (*Z*)-1-phenyl-2-trimethylsilyl- (**5a**) or (*Z*)-1,2-bis(trimethylsilyl)-3-(2-iodovinyl)cyclopropene (**5b**) and addition to either Vaska's or Vaska-type complexes generated iridabenzvalenes (**9**, **14**, **17**), iridabenzenes (**10**, **18**), and/or cyclopentadienyl complexes (**11**, **15**, **19**), depending on both the substituents on the C_5 framework and the phosphine ligands on Ir. Specifically, the reaction of **5a** with Vaska's complex afforded a mixture of **9**, **10**, and **11**. Heating this mixture to 75 °C converted **9** and **10** to **11**. NMR studies at 75 °C showed that samples of **9** isomerize to **11** in high yield and generate regioisomeric iridabenzene **12** as an intermediate. The reaction of **5b** with Vaska's complex produced benzvalene **14** as the sole product. Complex **14** transformed completely to cyclopentadienyliridium complex **15** at 75 °C with no benzene intermediate detectable by NMR spectroscopy. The reaction of cyclopropene **5a** with Vaska-type complexes containing alkylphosphines of varying cone angles yielded only benzvalene complexes, which either rearranged or decomposed depending upon the extent of heating. A hybrid-DFT computational study was carried out to investigate reactivity differences between phenyl and trimethylsilyl iridabenzvalenes, regioselective rearrangement of **9**, and the unexpected stability/instability of **14**/**16**. These calculations rationalize the sometimes contradictory experimental results.

Introduction

Metallabenzenes are six-membered metallacycles analogous to benzene where one CH unit has been replaced by an isoelectronic transition metal fragment (ML_n).[1] Originally postulated to be stable species by Thorn and Hoffman in their seminal paper in 1979,[2] the first unambiguous isolation of a metallabenzene was reported by Roper et al. just three years later.[3] In the subsequent two decades since their initial proposal, about 30 varieties of metalla-aromatic molecules were synthesized and/or characterized. Although most of the metallacycles prepared were isolated examples, a majority exhibited structural and spectroscopic properties normally associated with aromatic systems, such as ring planarity, delocalized bonding, and deshielded proton NMR chemical shifts.[1]

Research into aromatic metallacycles has undergone a major expansion since 2000.[4] A wide variety of new metallabenzenes,

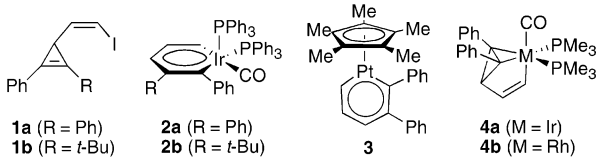

1a (R = Ph) **1b** (R = *t*-Bu) **2a** (R = Ph) **2b** (R = *t*-Bu) **3** **4a** (M = Ir) **4b** (M = Rh)

encompassing new synthetic methods[5] and new metal centers,[6] are now available. New aromatic metallacycle topologies[7] and constitutional isomers[8] have been isolated and characterized. In 1999 we introduced a new route to directly access the

* Corresponding authors. Experimental section: E-mail: haley@uoregon.edu. Fax: 541-346-0487. Phone: 541-346-0456. Computational section: E-mail: kimb@oci.unizh.ch. Fax: 41-1-635-6812. Phone: 41-1-635-4201.

§ Metallabenzenes and Valence Isomers 9. For Part 8, see ref 9b.

† University of Oregon.

‡ University of Zürich.

University of California, Los Angeles.

(1) Bleeke, J. R. *Chem. Rev.* **2001**, *101*, 1205−1227.

(2) Thorn, D. L.; Hoffman, R. *Nouv. J. Chim.* **1979**, *3*, 39−45.

(3) (a) Elliott, G. P.; Roper, W. R.; Waters, J. M. *J. Chem. Soc., Chem. Commun.* **1982**, 811−813. See also: (b) Elliott, G. P.; McAuley, N. M.; Roper, W. R. *Inorg. Synth.* **1989**, *26*, 184−189. (c) Rickard, C. E. F.; Roper, W. R.; Woodgate, S. D.; Wright, L. J. *J. Organomet. Chem.* **2001**, *623*, 109−115.

(4) (a) Landorf, C. W.; Haley, M. M. *Angew. Chem., Int. Ed.* **2006**, *45*, 3914−3936. (b) Wright, L. J. *Dalton Trans.* **2006**, 1821−1827.

(5) *Inter alia:* (a) Gilbertson, R. D.; Weakley, T. J. R.; Haley, M. M. *J. Am. Chem. Soc.* **1999**, *121*, 2597−2598. (b) Xia, H. P.; He, G. M.; Zhang, H.; Wen, T. B.; Sung, H. H. Y.; Williams, I. D.; Jia, G. C. *J. Am. Chem. Soc.* **2004**, *126*, 6862−6863. (c) Chin, C. S.; Lee, H. *Chem.−Eur. J.* **2004**, *10*, 4518−4522. (d) Alvarez, E.; Paneque, M.; Poveda, M. L.; Rendon, N. *Angew. Chem., Int. Ed.* **2006**, *45*, 474−477. (e) Hung, W. Y.; Zhu. J.; Wen, T. B.; Yu, K. P.; Sung, H. H. Y.; Williams, I. D.; Lin, Z. Y.; Jia, G. C. *J. Am. Chem. Soc.* **2006**, *128*, 13742−13752.

(6) (a) Jacob, V.; Weakley, T. J. R.; Haley, M. M. *Angew. Chem., Int. Ed.* **2002**, *41*, 3470−3473. (b) Zhang, H.; Xia, H. P.; He, G. M.; Wen, T. B.; Gong, L.; Jia, G. C. *Angew. Chem., Int. Ed.* **2006**, *45*, 2920−2923. (c) Zhang, H.; Feng, L.; Gong, L.; Wu, L.; He, G.; Wen, T.; Xia, H. *Organometallics* **2007**, *26*, 2705−2713.

(7) (a) Wen, T. B.; Zhou, Z. Y.; Jia, G. *Angew. Chem., Int. Ed.* **2001**, *40*, 1951−1954. (b) Paneque, M.; Posadas, C. M.; Poveda, M. L.; Rendon, N.; Salazar, V.; Oñate, E.; Mereiter, K. *J. Am. Chem. Soc.* **2003**, *125*, 9898−9899. (c) Clark, G. R.; Johns, P. M.; Roper, W. R.; Wright, L. J. *Organometallics* **2006**, *25*, 1771−1777. (d) Bierstedt, A.; Clark, G. R.; Roper, W. R.; Wright, L. J. *J. Organomet. Chem.* **2006**, *691*, 3846−3852. (e) Clark, G. R.; Lu, G.-L.; Roper, W. R.; Wright, L. J. *Organometallics* **2007**, *26*, 2167−2177.

10.1021/om700336d CCC: $37.00
Publication on Web 07/03/2007

Scheme 1

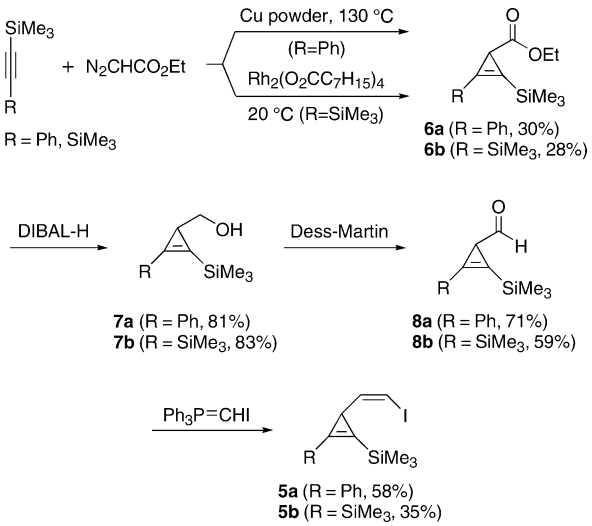

metallabenzene manifold using suitably substituted 3-vinylcyclopropenes (e.g., **1a**).[5a] Lithium−halogen exchange and subsequent addition to various metal complexes have resulted in the preparation of a variety of iridabenzenes (e.g., **2a**)[9] and platinabenzenes (e.g., **3**),[6a,10] as well as the formation and characterization of iridabenzvalenes (e.g., **4a**)[9,11] and rhodabenzvalenes (e.g., **4b**),[12] the first metallabenzene valence isomers. We extended this novel synthetic route to cyclopropene ligands with alkyl substituents (e.g., **1b**) and found that iridabenzvalene rearrangement to the corresponding benzene was regioselective (e.g., **2b**).[9b] To expand this chemistry further, we present herein the results from the reaction of mono- and bis-(trimethylsilyl)-substituted cyclopropenes with Vaska's and Vaska-type complexes, the former briefly described in our initial communication.[13] The reactions generate the corresponding iridabenzvalene, iridabenzene, and/or η^5-cyclopentadienyliridium complexes depending upon the exact ring substituents, phosphine ligands, and reaction conditions. In addition, we have performed a detailed DFT computational analysis to help explain the unusual experimental results.

Results and Discussion

Cyclopropene Ligand Synthesis. The straightforward preparation of the (Z)-1,2-disubstituted-3-iodovinylcyclopropene ligands **5a**,**b** is shown in Scheme 1. The reaction of phenyl(trimethylsilyl)acetylene with ethyl diazoacetate, which was modified by using Cu powder instead of a Rh complex as the catalyst, afforded ester **6a** in an improved 30% yield (lit.[14] 11% yield).

Scheme 2

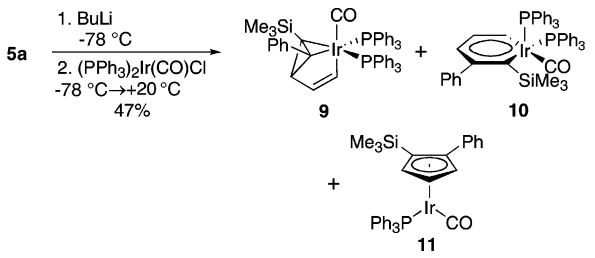

Ester **6b** was prepared according to the literature[15] via Rh catalysis because the Cu modification with bis(trimethylsilyl)-acetylene instead yielded the pyrazole [3+2] cycloadduct as the major product. Reduction of the esters with DIBAL-H gave compounds **7a** and **7b**,[15b] which were subsequently oxidized with Dess−Martin periodinane[16] to produce **8a** and **8b**.[15b] Wittig reaction with $Ph_3P{=}CHI$[17] furnished ligands **5a**,**b** with high stereoselectivity (>15:1 *Z*:*E*).

Reaction of Ligand 5a with Vaska's Complex. The reaction of cyclopropene **5a** with $(PPh_3)_2Ir(CO)Cl$ is shown in Scheme 2.[13] Lithium−halogen exchange at low temperature followed by addition of Vaska's complex and warming to ambient temperature resulted in a mixture of products, which after chromatography gave **9**, **10**, and **11** in a 10:2:3 ratio. Complexes **9** and **11** could be isolated independently by treating the mixture with MeI (removing **10** and **11** as polar salts[18]) and by heating the mixture (*vide infra*), respectively; nevertheless, samples of **10** always contained significant amounts of either **9** or **11**. All compounds were identified by NMR spectroscopic data, which are similar to those of diphenyl analogue **2** and related structures. The asymmetry of benzvalene **9** was indicated by two sets of downfield proton resonances attributed to the PPh_3 ligands and two different C resonances (δ 75.8, 55.5 ppm) of the complexed cyclopropenyl double bond. It is noteworthy that iridacycle **9** forms as the major product of this reaction, whereas the corresponding diphenyl-substituted molecule from Vaksa's complex (**4a**, where the phosphines are PPh_3) is never observed.

In an attempt to prepare a pure sample of **10**, we heated a C_6D_6 solution of **9** at 75 °C for 24 h. Although valence isomerization to yield **10** was the expected transformation, ^{1}H NMR analysis of the reaction mixture showed exclusive and essentially quantitative formation of **11**. This result is surprising given the ease with which benzvalene **4** can be converted to the corresponding iridabenzene.[11] Closer inspection of the thermal chemistry of these complexes showed multiple transformations. Analysis of a C_6D_6 solution of **9** heated at 75 °C for 1 h revealed, in addition to unreacted **9** and a small amount of **11**, the characteristic ^{1}H NMR signals for an iridabenzene. These resonances, however, were at 10.85 and 8.78 ppm and did not belong to **10** (10.45 and 8.14 ppm), thus suggesting the formation of a different iridabenzene (**12**, Scheme 3). The assignment of **12** as the regioisomer depicted in Scheme 3 is based on ^{1}H−^{29}Si gHMQC NMR experiments, which indicated that the *para* proton at 8.78 ppm is coupled to a silicon nucleus. Careful monitoring of the reaction showed that the concentration of **12** peaked after 8−10 h and then steadily decreased.

(8) Barrio, P.; Esteruelas, M. A.; Oñate, E. *J. Am. Chem. Soc.* **2004**, *126*, 1946−1947.
(9) (a) Gilbertson, R. D.; Lau, T. L. S.; Lanza, S.; Wu, H. P.; Weakley, T. J. R.; Haley, M. M. *Organometallics* **2003**, *22*, 3279−3289. (b) Wu, H. P.; Weakley, T. J. R.; Haley, M. M. *Chem.−Eur. J.* **2005**, *11*, 1191−1200.
(10) Landorf, C. W.; Jacob, V.; Weakley, T. J. R.; Haley, M. M. *Organometallics* **2004**, *23*, 1174−1176.
(11) Gilbertson, R. D.; Weakley, T. J. R.; Haley, M. M. *Chem.−Eur. J.* **2000**, *6*, 437−441.
(12) Wu, H.-P.; Weakley, T. J. R.; Haley, M. M. *Organometallics* **2002**, *21*, 4320−4322.
(13) Wu, H.-P.; Weakley, T. J. R.; Haley, M. M. *Organometallics* **2002**, *21*, 2824−2826.
(14) (a) Müller, P.; Gränicher, C. *Helv. Chim. Acta* **1993**, *76*, 521−534. (b) Dolgil, I. E.; Okonnishnikova, G. P.; Nefedov, O. M. *Akad. Nauk SSSR, Ser. Khim.* **1979**, *4*, 822−829.
(15) (a) Kohn, D. W.; Chen, P. *J. Am. Chem. Soc.* **1993**, *115*, 2844−2848. (b) Maier, G.; Hoppe, M.; Reisenauer, H. P.; Kruger, C. *Angew. Chem., Int. Ed. Engl.* **1982**, *21*, 437.
(16) Dess, D. B.; Martin, J. C. *J. Am. Chem. Soc.* **1991**, *113*, 7277−7287.
(17) (a) Stork, G.; Zhao, K. *Tetrahedron Lett.* **1989**, *30*, 2173−2174. (b) Bestmann, H. J.; Rippel, H. G.; Dostalek, R. *Tetrahedron Lett.* **1989**, *30*, 5261−5262.
(18) Wang, D.; Angelici, R. J. *Inorg. Chem.* **1996**, *35*, 1321−1331.

Scheme 3

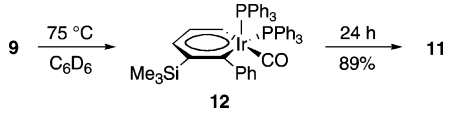

Scheme 4

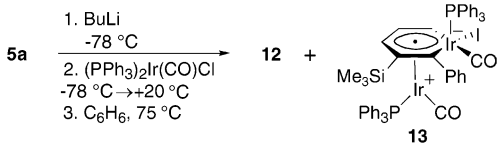

Benzvalene **9** was completely consumed after 15 h, with total conversion of **9** (and **12**) to **11** after 24 h at 75 °C in 89% isolated yield. Heating the purified mixture of **9**−**11** afforded similar results. After 1 h, the resonances of **10** had disappeared and been replaced by signals for **12**. The intensity of the signals for **9** and **11** had decreased and increased, respectively. The disappearance of **9** and **12** progressed as described above upon further heating. After 24 h, conversion to **11** (with concomitant formation of PPh_3) was complete with a color change from red-brown to yellow. Attempts to retard formation of **11** (and thus potentially increase amounts of **10** and/or **12**) by addition of excess PPh_3, known to inhibit phosphine dissociation in iridabenzenes,[19] were not successful. The computational results (*vide infra*) will show that benzene **12** is the preferred regioisomer; thus, the origins of **10** are uncertain.

To "simplify" the preparation of **11**, the crude mixture of **9**−**11** obtained after reaction workup was heated in benzene at 75 °C for 24 h (Scheme 4). Rapid chromatography gave **11** as the major product (ca. 40%) along with a new red byproduct, complex **13** (ca. 5%), which is moderately air-stable as a solid at 0 °C. Spectroscopic data indicated that **13** contained two iridium atoms with different coordination spheres: ^{13}C NMR data exhibited two lower field resonances at 179.96 and 174.82 ppm, attributed to two CO ligands. As then expected, two carbonyl bands at 2026 and 1950 cm^{-1} were observed in the IR spectrum. The ^{31}P NMR spectrum showed two sets of PPh_3 resonance peaks at 17.00 and 11.06 ppm. ^1H NMR spectra showed the three C*H* resonances at 6.07, 5.81, and 5.16 ppm, significantly upfield compared with the corresponding C*H* proton resonances (10.85 and 8.78 ppm, with one peak masked by the Ph multiplets) in iridabenzene **12**. These latter data are very common for η^6-coordinated metallabenzene complexes[1,19] and thus suggested that **13** is a dinuclear complex in which the iridabenzene is coordinated to a second iridium fragment.

The exact structure of **13** (Figure 1) was confirmed by X-ray diffraction of crystals obtained from Et_2O/hexane overnight at −30 °C. Selected bond lengths and bond angles are listed in Figure 1. The crystal structure of **13** confirms our expectations of two iridium centers, with an Ir−Ir bond distance of 2.743(1) Å, comparable to previously determined Ir−Ir bond lengths (ca. 2.70−2.72 Å).[20] Complex **13** can be formulated as a zwitterionic species with 18 electrons on both iridium centers.[21] Ir1 in the iridabenzene ring is bound to CO, PPh_3, and I ligands, whereas

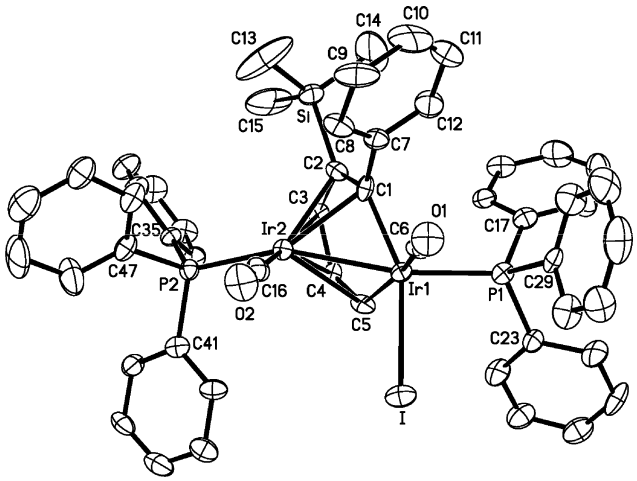

Figure 1. Molecular structure of diiridium complex **13**. The thermal ellipsoids are drawn at the 30% probability level. Selected bond lengths (Å) and angles (deg): Ir1−Ir2 2.744(1), Ir1−I 2.792(1), Ir1−P1 2.283(4), Ir1−C1 2.066(13), Ir1−C5 2.027(13), Ir1−C6 1.922(15), Ir2−P2 2.290(3), Ir2−C16 1.831(16), Ir2−C1 2.287(13), Ir2−C2 2.358(12), Ir2−C3 2.271(11), Ir2−C4 2.337(12), Ir2−C5 2.397(13), Si−C2 1.915(14), C1−C2 1.415(17), C2−C3 1.442(17), C3−C4 1.447(17), C4−C5 1.389(17); I−Ir1−P1 93.73(9), I−Ir1−C1 156.0(3), I−Ir1−C5 86.3(4), I−Ir1−C6 85.4(4), P1−Ir1−C1 110.2(3), P1−Ir1−C5 104.4(4), P1−Ir1−C6 91.2(4), C1−Ir1−C5 89.4(5), C5−Ir1−C6 162.9(5), P2−Ir2−C16 89.0(4), Ir1−C1−C2 129(1), C1−C2−C3 121(1), C2−C3−C4 126(1), C3−C4−C5 125(1), C4−C5−Ir1 128.4(9).

Ir2 is bound to CO and PPh_3 ligands as well as η^6-bound to the iridabenzene backbone, with an average Ir2−C_{ring} distance of 2.33 Å. The iridabenzene ring is nearly planar with an average deviation of 0.039 Å, which is slightly larger than for free iridabenzene **2a** (0.024 Å).[5a] Ir1−C1 and Ir1−C5 (2.066(13) and 2.027(13) Å) as well as the C−C bond distances in the ring (ranging from 1.389 to 1.447 Å) are very close to each other, respectively, but are slightly longer than those in uncoordinated **2a** (1.334−1.410 Å).[5a] These data nonetheless suggest that coordinated iridabenzene **13** possesses a delocalized aromatic π-system. The torsion angle of Ir1−C1−C2−C3 (13°) is much larger than that in iridabenzene **2a** (−2°) and is likely caused by steric repulsion between the bulky $SiMe_3$ and Ph substituents. The longer Ir1−C6 bond distance (1.922(15) Å) versus Ir2−C16 (1.831(16) Å) may be attributed to stronger back-bonding from Ir2 to the CO ligand and reflects the electron difference of the coordination environments around both Ir centers.

The structure of complex **13** shows that the positions of the $SiMe_3$ and Ph groups are the same as those in iridabenzene regioisomer **12**, the most likely precursor of **13**. Attempts to improve the yield of **13** by fine-tuning conditions, such as adding excess Vaska's complex or excess iodide to the crude reaction mixture before heating, were unsuccessful. While it is not entirely clear how the [Ir(PPh_3)(CO)] and [Ir(CO)I(PPh_3)] fragments in complex **13** are generated, a likely explanation is that during the heating step in which it forms, iridabenzene **12** is intercepted by an adventitious Ir(I) fragment (possibly via **11**); subsequent phosphine replacement with I^- results in a neutral, isolable species.

Reaction of Ligand 5b with Vaska's Complex. If switching from **1** to **5a** in iridabenzene synthesis led to such a more complex reaction manifold, we were very curious to see how inclusion of two $SiMe_3$ substituents on **5b** would alter the reactivity with Vaska's complex. Under identical conditions,

(19) Bleeke, J. R.; Behm, R; Xie, Y.-F.; Chiang, M. Y.; Robinson, K. D.; Beatty, A. M. *Organometallics* **1997**, *16*, 606−623.

(20) (a) Angoletta, M.; Ciant, G.; Manassero, M.; Sansoni, M. *J. Chem. Soc., Chem. Commun.* **1973**, 789−790. (b) Rausch, M. D.; Gastinger, R. G.; Hardner, S. A.; Brown, R. K.; Wood, J. S. *J. Am. Chem. Soc.* **1977**, *99*, 7870−7876. (c) Browning, J.; Dixon, K. R.; Meanwell, N. J. *Inorg. Chim. Acta* **1993**, *213*, 171−175.

(21) A similar zwitterionic structure was proposed for a ruthenabenzene η^6-coordinated to a second Ru fragment; see: Lin, W.; Wilson, S. R.; Girolami, G. S. *J. Chem. Soc., Chem. Commun.* **1993**, 284−285.

Scheme 5

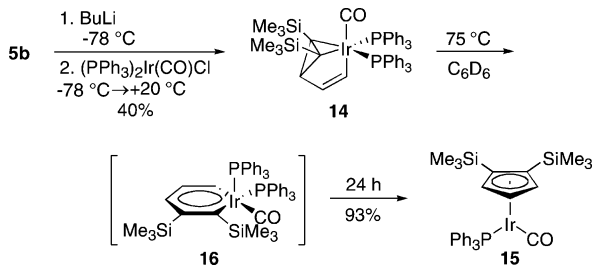

the reaction produced iridabenzvalene **14** exclusively (Scheme 5), as evidenced by the ^{1}H NMR spectrum of the crude mixture. Compound **14** was purified by recrystallization in Et_2O/hexane overnight at −30 °C. It is stable for months as a solid and in solution at room temperature under an N_2 atmosphere. Complex **14** is in fact the most stable PPh_3-containing benzvalene yet produced, requiring heating in C_6D_6 solution at 75 °C for 20 h for complete conversion to cyclopentadienyl complex **15**; only 13% transformation was observed after 6 h at 50 °C. Surprisingly, no iridabenzene intermediate was ever observed in the ^{1}H NMR spectra during heating. While it is reasonable to assume that arene **16** forms by isomerization of **14** based on the previous studies from our lab,[9,11] **16** must be short-lived and thus rearranges readily to **15**. Interestingly, all attempts to protiodesilylate pure **9** or **14**, thus yielding either a mono- or unsubstituted metallabenzene backbone, were unsuccessful.

The ^{1}H NMR spectrum of **14** showed the typical peaks for an iridabenzvalene skeleton at 6.47, 5.84, and 2.68 ppm, with the upfield shift of the *H3* resonance attributed to the influence of the two $SiMe_3$ groups (δ_{H3} 3.08 ppm in **9**). The C_S-symmetry of the complex was confirmed by NMR: one set of Ph peaks for the PPh_3 ligand was observed in the proton spectrum, and the ^{31}P NMR spectrum showed only one resonance at 3.09 ppm. The IR spectrum possessed a strong CO absorption band at 1973 cm^{-1}. The structure of complex **14** was further confirmed by single-crystal X-ray diffraction; the molecular structure and selected bond lengths and angles are given in Figure 2. The X-ray data confirm a symmetrical plane defined by Ir−C3−C4−C5, the midpoint between C1−C2, and the CO group. Complex **14** has a trigonal bipyramidal configuration similar to diphenyl analogue **4a**.[9,11] The C1−C2 bond distances in **14** (1.446 Å) and **4a** (1.447 Å) are essentially identical. Additionally, the C5−Ir−C6 bond angle (172.6°) is smaller than in **4a** (178.9°), while the Ir−C1 and Ir−C2 bond distances (2.173, 2.189 Å for **14**) are slightly longer (2.146, 2.143 Å for **4a**), data reflecting the steric repulsion between the bulky $SiMe_3$ groups and the PPh_3 ligands.

Reaction of Ligand 5a with Vaska-Type Complexes. Reaction of cyclopropene **5a** with Vaska-type complexes containing alkylphosphines with different cone angles was next studied. ^{1}H NMR spectra of crude reaction mixtures indicated that benzvalenes **17a**−**e** are the sole isolable product (Scheme 6 and Table 1). Unlike **9**, complexes **17a**−**e** underwent significant decomposition on attempted chromatographic purification. Instead, treatment of the mixture with Bu_4NF (in which unreacted or protiodeiodonated **5a** could be desilylated and the resultant unstable, volatile cyclopropene byproducts removed) afforded 42−85% yields of **17a**−**e** as pale yellow oils, which were stable at room temperature. The ^{1}H NMR spectra of **17a**−**e** showed the characteristic resonance of the sp^3 C*H* group at 3.12−3.46 ppm, and the CO absorption band in the IR spectra was in the range 1986−1965 cm^{-1}.

The thermal stabilities of iridabenzvalenes **17a**−**e** were investigated, and their rearrangement and decomposition found

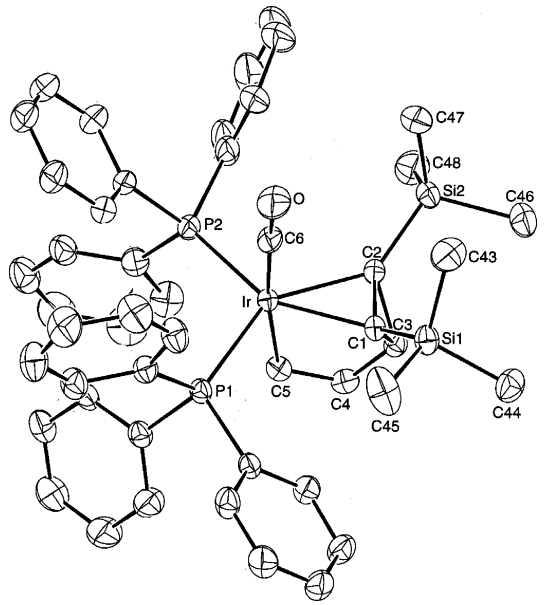

Figure 2. Molecular structure of iridabenzvalene **14**. The thermal ellipsoids are drawn at the 30% probability level. Selected bond lengths (Å) and angles (deg): Ir−P1 2.367(1), Ir−P2 2.381(1), Ir−C1 2.173(4), Ir−C2 2.189(4), Ir1−C5 2.074(4), Ir−C6 1.882(5), Si1−C1 1.858(4), Si2−C2 1.941(4), O−C6 1.149(5), C1−C2 1.446(6), C1−C3 1.539(6), *C*2−C3 1.543(6), C3−C4 1.457(6), C4−C5 1.330(5); P1−Ir−P2 106.47(4), P1−Ir−C1 105.0(1), P1−Ir−C5 83.8(1), P1−Ir−C6 99.1(1), P2−Ir−C2 109.2(1), P2−Ir−C5 93.4(1), P2−Ir−C6 92.2(1), C1−Ir−C2 38.7(2), C5−Ir−C6 172.6(2), Ir−C1−Si1 134.0(2), Ir−C1−*C*2 71.2(2), Ir−C1−C3 96.5(2), Si−C1−C2 130.4(4), C2−C1−C3 62.2(3), Ir−C2−Si2 140.8(2), Ir−C2−C1 70.0(2), Ir−C2−C3 95.8(3), Si2−C2−C1 137.4(3), Si2−C2−C3 120.9(3), C1−C2−C3 61.9(3), C1−C3−C2 56.0(3), C1−C3−C4 117.8(4), C2−C3−C4 117.0(4), C3−C4−C5 115.2(4), Ir−C5−C4 112.3(3).

Scheme 6

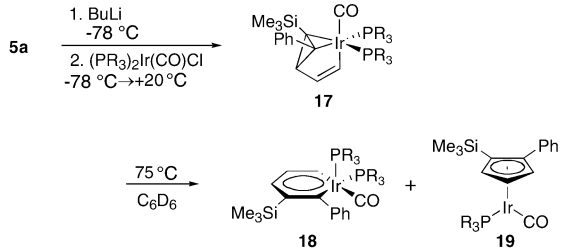

PR_3 = PMe_3 **(a)**, PMe_2Ph **(b)**, PEt_3 **(c)**, $PMePh_2$ **(d)**, P*i*-Bu_3 **(e)**

Table 1. Reaction of Lithiated 5a with Vaska-Type Complexes and Subsequent Heating of 17a−e in C_6D_6 Solution at 75 °C

entry	yield of **17** (%)	PR_3	cone angle (deg)[a]	heating time (h)	ratio **17**:**18**:**19**
17a	50	PMe_3	118	24	100:0:0
17b	85	PMe_2Ph	122	24	>99:trace:0
17c	42	PEt_3	132	24	100:0:0
17d	59	$PMePh_2$	136	24	59:23:18
				90	0:0:100
17e	63	P*i*-Bu_3	143	24	0:0:100[b]
9		PPh_3	145	24	0:0:100[c]

[a] Reference 22. [b] No **18e** was observed. [c] Ratio of **9**:**12**:**11**.

to depend upon the cone angle of the phosphine ligands[22] and the temperature applied. The distribution of complexes **17**, **18**, and **19** in the thermal interconversion is summarized in Table

(22) Tolman, C. A. *Chem. Rev.* **1977**, *77*, 313−348.

Scheme 7

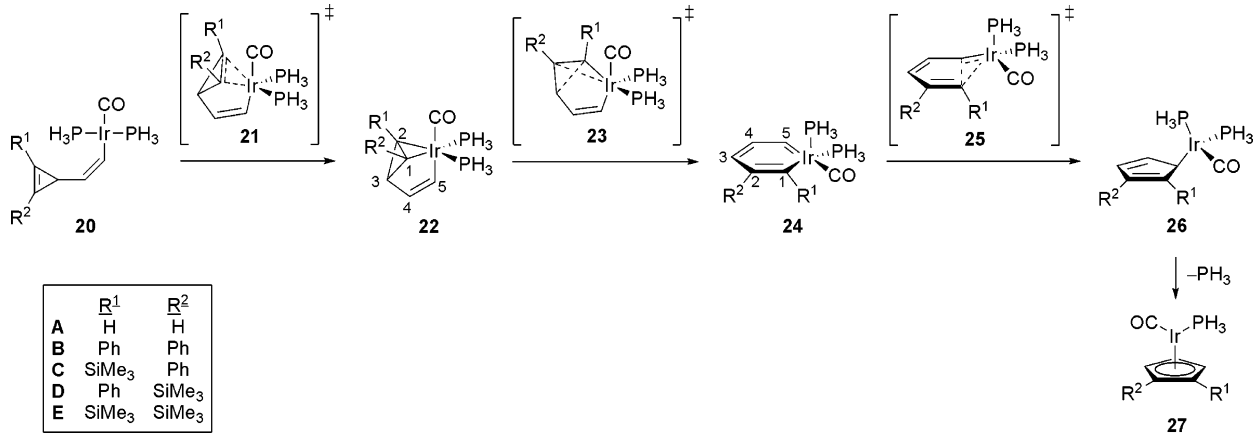

	R^1	R^2
A	H	H
B	Ph	Ph
C	$SiMe_3$	Ph
D	Ph	$SiMe_3$
E	$SiMe_3$	$SiMe_3$

1. Whereas complex **17a** was stable at 75 °C for 24 h, at 100 °C in toluene-d_8 it gradually decomposed with trace formation of iridabenzene **18a** and, more importantly, with no evidence of formation of **19a**. Iridabenzvalenes **17b**,**c** exhibited similar behavior. Conversely, thermolysis of **17e** afforded cyclopentadienyl **19e** cleanly without intermediate iridabenzene **16e** being observed, analogous to the transformation of **14** → **15**. Benzvalene **17d** was the sole species to give a mixture of complexes after 24 h at 75 °C, yielding a 59:23:18 ratio of **17d**, **18d**, and **19d**, and the only system to generate an iridabenzene in an appreciable amount. Conversion to exclusively **19d** was accomplished by protracted heating (90 h). It is doubtful that increasing the cone angle sterics by 4° from PEt_3 to $PMePh_2$ is solely responsible for inducing the rearrangement of the **d** series. As we have previously observed,[9] the electron-donating ability of the phosphine ligands plays a significant role in benzvalene stability. PEt_3 with three alkyl groups is considerably more donating than $PMePh_2$; thus, the more electron-rich Ir center in **17c** back-bonds more efficiently and stabilizes the benzvalene. Similarly, the cone angle of P*i*-Bu_3 is very close to that of PPh_3, yet the reaction with (P*i*-Bu_3)$_2$Ir(CO)Cl produced only **17e** at room temperature, in stark contrast to the three products generated in the reaction with Vaska's complex (**9**−**11**) under the same conditions.

Computational Studies

In this section we report a computational investigation for the determination of the stability of phenyl- and trimethylsilyl-substituted iridabenzvalenes and iridabenzenes. We employed the hybrid B3LYP functional[23] with the LANL2DZ[24] (ECP) basis set for geometry optimizations and thermal corrections, and the 6-311+G(2d,p)/LANL2DZ basis set for energies as implemented in the Gaussian 03 suite of programs.[25] Stuttgart−Dresden effective core potentials resulted in nearly identical geometries.[26] All stationary points were verified as minima or first-order saddle points by full calculation of the Hessian and a harmonic frequency analysis. Our model system employs phosphine ligands in place of triphenylphosphine ligands on the iridium metal. This was done for several reasons. First, the scope and primary purpose of this study was to investigate electronic effects exerted by phenyl and trimethylsilyl groups. Second, the previous section showed convincingly that the well-known electronic effects of PR_3 groups are more important than steric influences. Last, calculations with triphenylphosphine ligands are still computationally unfeasible for full Hessian characterization (∼1000 basis functions). Constrained optimizations (freezing breaking/forming bonds) on test cases were performed and showed no significant steric interaction with triphenylphosphine groups in the transition states.

In 2004, Martin and co-workers published a series of introductory computational studies into metallabenzene chemistry using the MPW1K density functional.[27] Five significant results were proposed and are summarized here. (1) Metallabenzenes are formed from metallabenzvalene intermediates through Ir−C and C−C bond breaking. The alternative route through a Dewar−metallabenzene species is significantly higher in energy. (2) Metallabenzenes rearrange through a carbene migration reaction with a three-atom-centered asymmetric (two nonequivalent Ir−C bond lengths) transition state that couples the C−C bond by pinching two CH groups together. To accommodate the C−C bond formation, the Ir metal center and ligands are distorted from planarity. (3) The C−C coupling is followed by phosphine ligand loss to generate the η^5-cyclopentadienyl complex in a generally exergonic process. (4) Metal ligands may alter the barrier height and stability of metallabenzenes. For example, changing from (C_5H_5Ir)(PH_3)$_3$ to (C_5H_5-

(23) The B3LYP functional has been successful for a variety of organometallic reactions; see for example: (a) Strassner, T.; Taige, M. A. *J. Chem. Theory Comput.* **2005**, *1*, 848−855. (b) Oxidative addition: de Jong, G. T.; Bickelhaupt, F. M. *J. Chem. Theory Comput.* **2006**, *2*, 322−335. (c) de Jong, G. T.; Bickelhaupt, F. M. *J. Phys. Chem. A* **2005**, *109*, 9685−9699. (d) de Jong, G. T.; Geerke, D. P.; Diefenbach, A.; Bickelhaupt, F. M. *Chem. Phys.* **2005**, *313*, 261−270. (e) de Jong, G. T.; Geerke, D. P.; Diefenbach, A.; Solà, M.; Bickelhaupt, F. M. *J. Comput. Chem.* **2005**, *26*, 1006−1020.

(24) Hay, P. J.; Wadt, W. R. *J. Chem. Phys.* **1985**, *82*, 270.

(25) Frisch, M. J.; Trucks, G. W.; Schlegel, H. B.; Scuseria, G. E.; Robb, M. A.; Cheeseman, J. R.; Montgomery, J. A., Jr.; Vreven, T.; Kudin, K. N.; Burant, J. C.; Millam, J. M.; Iyengar, S. S.; Tomasi, J.; Barone, V.; Mennucci, B.; Cossi, M.; Scalmani, G.; Rega, N.; Petersson, G. A.; Nakatsuji, H.; Hada, M.; Ehara, M.; Toyota, K.; Fukuda, R.; Hasegawa, J.; Ishida, M.; Nakajima, T.; Honda, Y.; Kitao, O.; Nakai, H.; Klene, M.; Li, X.; Knox, J. E.; Hratchian, H. P.; Cross, J. B.; Adamo, C.; Jaramillo, J.; Gomperts, R.; Stratmann, R. E.; Yazyev, O.; Austin, A. J.; Cammi, R.; Pomelli, C.; Ochterski, J. W.; Ayala, P. Y.; Morokuma, K.; Voth, G. A.; Salvador, P.; Dannenberg, J. J.; Zakrzewski, V. G.; Dapprich, S.; Daniels, A. D.; Strain, M. C.; Farkas, O.; Malick, D. K.; Rabuck, A. D.; Raghavachari, K.; Foresman, J. B.; Ortiz, J. V.; Cui, Q.; Baboul, A. G.; Clifford, S.; Cioslowski, J.; Stefanov, B. B.; Liu, G.; Liashenko, A.; Piskorz, P.; Komaromi, I.; Martin, R. L.; Fox, D. J.; Keith, T.; Al-Laham, M. A.; Peng, C. Y.; Nanayakkara, A.; Challacombe, M.; Gill, P. M. W.; Johnson, B.; Chen, W.; Wong, M. W.; Gonzalez, C.; Pople, J. A. *Gaussian 03*, Revision B.05; Gaussian, Inc.: Pittsburgh, PA, 2003.

(26) Fuentealba, P.; Preuss, H.; Stoll, H.; von Szentpaly, L. *Chem. Phys. Lett.* **1982**, *89*, 418−422.

(27) (a) Iron, M. A.; Martin, J. M. L.; van der Boom, M. E. *J. Am. Chem. Soc.* **2003**, *125*, 13020−13021. (b) Iron, M. A.; Lucassen, A. C. B.; Cohen, H.; van der Boom, M. E.; Martin, J. M. L. *J. Am. Chem. Soc.* **2004**, *126*, 11699−11710. (c) See also: Zhu, J.; Jia, G.; Lin, Z. *Organometallics* **2007**, *26*, 1986−1995.

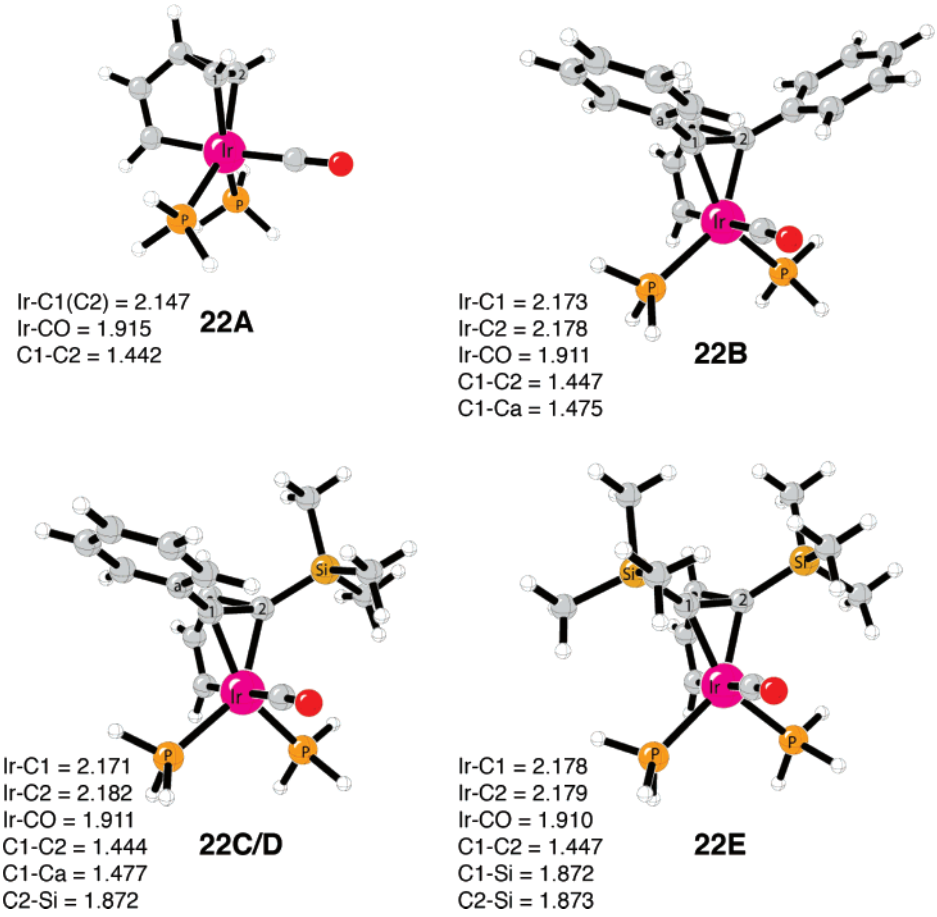

Figure 3. B3LYP minima for iridabenzvalenes **22A**−**E** (compounds **4a**, **9**, **14**).

Ir)$(PH_3)_2Cl_2$ lowers the $\Delta G^{\ddagger}$ from 44.4 kcal mol^{-1} to 35.2 kcal mol^{-1}. (5) Substitution on the hydrocarbon ring *para* to the metal fragment also affects the barrier height. A Hammett plot for *para*-NH_2-, OMe-, Cl-, COOH-, and NO_2-substituted (C_5H_5-Ir)$(PH_3)_3$ activation energies against σ^+ values indicated a reductive elimination mechanism, since electron-donating groups raise the barrier height for carbene migration, while electron-withdrawing groups lower the barrier height.

The purpose of the current hybrid-DFT study is threefold: (1) explore the reactivity differences between phenyl- and trimethylsilyl-substituted iridabenzvalenes and iridabenzenes; (2) investigate the regioselective rearrangement to the *meta*-(trimethylsilyl) iridabenzene **12** over the *ortho*-(trimethylsilyl) iridabenzene **10**; and (3) investigate the unexpected stability of iridabenzvalene **14** and instability of the bis(trimethylsilyl)-iridabenzene **16**. To this end, the stationary points along the minimum energy reaction pathway from iridacyclopropene complex **20** to the cyclopentadienyliridium complex **27** for **A**−**E**, where R_1 and R_2 = H, Ph, or $SiMe_3$, have been investigated (Scheme 7).

The reaction involving unsubstituted iridium σ-vinyl complex **20A** (R_1, R_2 = H) involves a symmetric transition state **21A**, with an activation free energy of 7.4 kcal mol^{-1}, that leads to the corresponding iridabenzvalene **22A**. In the cases of phenyl- and trimethylsilyl-substituted R_1 and R_2 groups, the potential energy surfaces for formation of the iridacyclopropane Ir−C bonds are flat with no well-defined transition state (see Supporting Information). The B3LYP iridabenzvalene structures **22A**−**E** are shown in Figure 3. The ΔG_{rxn} for **22A**, **B**, **C/D**, and **E** are −11.2, −3.1, −3.8, and −1.3 kcal mol^{-1}, respectively (Table 2), indicating relatively weak η^2-interactions for **22B**−**E**. The approximately 7 kcal mol^{-1} drop in reaction energy for **22B**−**E** compared to **22A** is due to longer Ir−C bond lengths, which range from 2.171 to 2.182 Å compared to 2.147 Å for **22A**, caused by the repulsion of the metal center and ligands with the phenyl and trimethylsilyl groups.

Table 2. B3LYP/6-311+G(2d,p)/LANL2DZ(ECP) Reaction Energies for Iridabenzvalenes 22A−E and Activation Energies for Rearrangement to Iridabenzenes[a]

species	R_1, R_2	ΔE[b]	ΔH[c]	ΔG[c]
22A	H, H	*−13.9*	*−14.2*	*−11.2*
23A	H, H	29.7 [15.8]	28.0 [13.8]	27.4 [16.2]
22B	Ph, Ph	*−5.8*	*−6.5*	*−3.1*
23B	Ph, Ph	21.9 [16.1]	20.2 [13.7]	21.1 [18.0]
22C	$SiMe_3$, Ph	*−6.0*	*−6.8*	*−3.8*
23C	$SiMe_3$, Ph	28.8 [22.8]	27.4 [20.6]	28.1 [24.3]
22D	$SiMe_3$, Ph	*−6.0*	*−6.8*	*−3.8*
23D	Ph, $SiMe_3$	27.7 [21.7]	26.1 [19.3]	27.5 [23.7]
22E	$SiMe_3$, $SiMe_3$	*−5.8*	*−6.5*	*−1.3*
23E	$SiMe_3$, $SiMe_3$	35.2 [29.4]	33.5 [27.0]	32.5 [31.2]

[a] Values relative to the iridium vinylcyclopropene complexes **20A**−**E** are bracketed. Reaction energies are italicized (kcal mol^{-1}). [b] ZPE-corrected. [c] Corrections done at 298 K.

As discussed previously, Iron et al. showed that the minimum energy pathway for transformation of iridabenzvalene to iridabenzene involves transition state **23**, where the Ir−C2 and C1−C3 bonds break along with twisting the C2 atom of the iridacyclopropane ring, to give the planar iridabenzene **24** (Scheme 7). Figure 4 shows the calculated transition states **23B**−**E**. The activation barriers corresponding to these transition states are reported in Table 2. For the unsubstituted benzvalene **23A**, the activation free energy is 27.4 kcal mol^{-1}. The 6.3 kcal mol^{-1} lowering of the $\Delta G^{\ddagger}$ for the bis(phenyl)benzvalene transition state **23B** (21.1 kcal mol^{-1}) compared to **23A** is due to a less stable iridabenzvalene complex **22B**. Barrier heights relative to

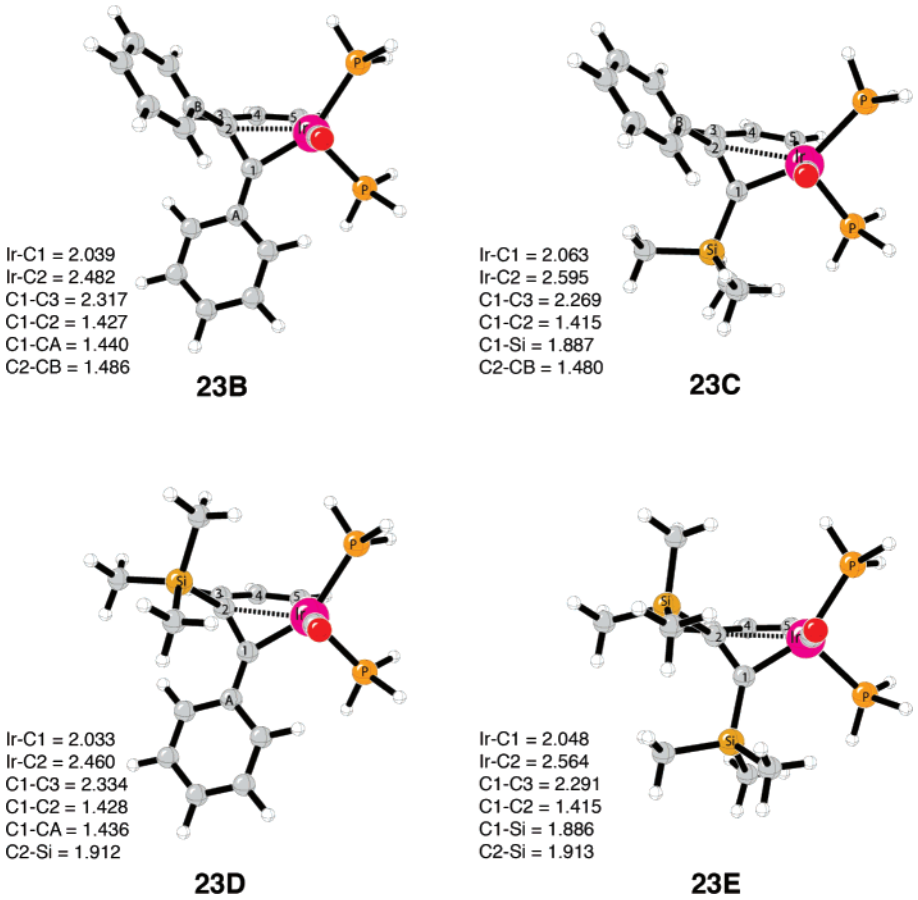

Figure 4. Transition states for iridacyclopropane ring opening of iridabenzvalenes.

the respective iridium vinylcyclopropene complexes for **23A** and **23B** are very close in energy (15.8 and 16.1 kcal mol^{-1}).

Benzvalene **22C/D** has the possibility to rearrange by breaking either the Ir−C1 or Ir−C2 bonds. Transition state **23C** reveals the *ortho*-$SiMe_3$ metallabenzene, whereas **23D** forms the *meta*-$SiMe_3$ metallabenzene. The $\Delta G^{\ddagger}$ values for **23C** and **23D** are 28.1 and 27.5 kcal mol^{-1}, respectively, about 6−7 kcal mol^{-1} higher than **23B**. Although **23D** is only favored by 0.6 kcal mol^{-1}, there is a substantial difference in its geometry compared to **23C**. The Ir−C2 bond length in **23D** is 2.460 Å, much shorter than 2.595 Å for **23C**. There is also a substantial difference in C1−C3 partial bond lengths, 2.334 versus 2.269 Å for **23D** and **23C**, respectively. The selectivity between **23C** and **23D** shows preference for breakage of the Ir−C bond with the $SiMe_3$ attached due to the ability of this group to stabilize through σ-donation. The extent of this effect is evident from the charges developed in the transition state. For **23C**, the C1 and C2 atoms have Mulliken charges of $-0.56e$ and $+0.78e$. The magnitudes of these charges are much larger than for **23D**, which are $+0.25e$ and $-0.29e$ for C1 and C2 atoms, respectively, where the trimethylsilyl group stabilizes the developing positive charge at the C2 atom position.

The barrier for rearrangement involving transition state **23E** is 32.5 kcal mol^{-1}, 11.4 kcal mol^{-1} higher than that involving the bis(phenyl)-substituted **23B** transition state. This large difference in activation free energy is likely the reason for the observed stability of compound **14**. The geometry of **23E** is similar to **23C**, with a long Ir−C2 partial bond length of 2.564 Å and C1−C3 partial bond length of 2.291 Å. The σ-donation of two trimethylsilyl groups, due to the low electronegativity of the silicon atom, is apparent from the transition state atomic charges, $-0.12e$ and $-0.60e$ for atoms C1 and C2.[28] Beyond the electronic effects of two $SiMe_3$ groups, there is also increased steric repulsion between these groups in the transition state. In **22E**, the nearest Si−Me/Si−Me interaction is 2.45 Å, while in **23E**, this decreases to 2.29 Å.

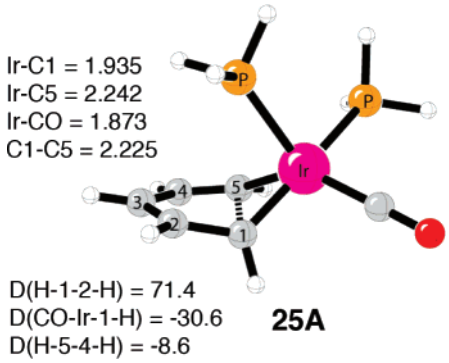

Figure 5. Transition state for C−C bond coupling of $(C_5H_5Ir)(PH_3)_2CO$.

We have also investigated the reactivity and substituent effects for the C−C bond coupling, referred to as a carbene migratory insertion, of **24A**−**E** to their corresponding η^1- and η^5-cyclopentadienyliridium complexes **26** and **27**. Figure 5 shows transition state **25A** for the unsubstituted iridabenzene $(C_5H_5Ir)(PH_3)_2CO$. The activation free energy is 41.8 kcal mol^{-1} and

(28) (a) Basindale, A. R.; Eaborn, C.; Walton, D. R. M.; Young, D. J. *J. Organomet. Chem.* **1969**, *20*, 49−56. (b) Cook, M. A.; Eaborn, C.; Walton, D. R. M. *J. Organomet. Chem.* **1970**, *24*, 293−299. (c) Campanelli, A. R.; Domenicano, A.; Ramondo, F. *J. Phys. Chem. A* **2003**, *107*, 6429−6440. (d) Schormann, M.; Garratt, S.; Bochmann, M. *Organometallics* **2005**, *24*, 1718−1724.

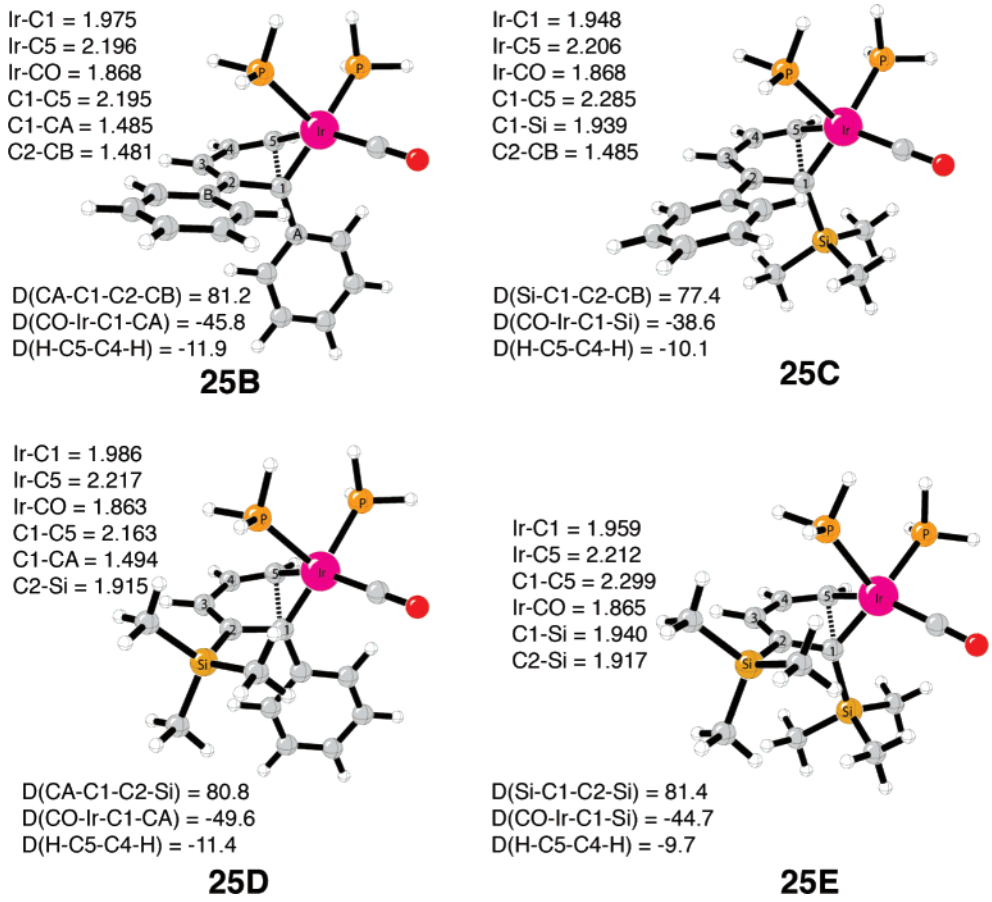

Figure 6. Transition states **25B**−**D** for C−C bond coupling of iridabenzenes **24B**−**D**.

the ΔG_{rxn} is −24.7 kcal mol^{-1} for rearrangement to the η^5-complex. **25A** shows the C1−C5 bond coupling via an Ir−C1−C5 three-centered transition state. The C1−C5 distance of iridabenzene **24A** is 2.751 Å and decreases to 2.225 Å in **25A**. Transition state **25A** is asymmetric, with two very different Ir−C bond lengths, 1.935 and 2.242 Å for the Ir−C1 and Ir−C5 bonds, respectively. As the reaction progresses toward the transition state from **24A**, which has two equivalent Ir−C bond lengths of 1.992 Å, the degeneracy is lifted and it becomes evident that the C5 position is more appropriately classified as a vinyl anion, while the C1 position is better classified as a metal−carbon double bond. This is also evident from the large dihedral angle difference between *D*(H−C1−C2−H) and *D*(H−C5−C4−H), 71.4° and −8.6°, respectively. The torquing motion at the C1−H center aligns the C1 p-orbital with the C5 vinyl anion orbital in the plane of the metallabenzene ring; therefore, π-interactions at C1 will directly influence bond formation, while C2−C5 substitution will affect bond formation indirectly.

Figure 6 shows the transition structures (**25B**−**E**) for C−C bond coupling of **24B**−**E**. Table 3 reports the B3LYP activation and reaction energetics for the reactions involving these transition states. The $\Delta G^{\ddagger}$ for bis(phenyl) **25B** is 28.5 kcal mol^{-1}, a 13.3 kcal mol^{-1} lower barrier than **25A** with no substitution. The $\Delta\Delta G^{\ddagger}$ for **25B** compared to **25A** is larger than the sum of single Ph substitution effects (see Supporting Information), indicating a synergetic lowering of the barrier due to ground state destabilization of iridabenzene **24B** from adjacent Ph groups and because the Ph groups are twisted compared to the metallabenzene ring system in the bis(phenyl) iridabenzenes. The torquing of the C1−Ph group in the transition state allows the C2−Ph group to be conjugated with the C2−C5 hydrocarbon ring fragment. This is reflected in the intermediate C2−CB bond length of 1.481 Å in **25B**. The torquing motion also allows the full effect of the Ph group at the C1 center, which has a larger influence on bond formation than substitution at the C2 position.

Table 3. B3LYP/6-311+G(2d,p)/LANL2DZ(ECP) Activation and Reaction Energies, Enthalpies, and Free Energies for C−C Coupling of 24A−E[a]

species	R_1, R_2	ΔE^b	ΔH^c	ΔG^c
25A	H, H	41.5 [1.6]	41.4 [1.0]	41.8 [4.0]
27A	H, H	*−14.3 [−54.2]*	*−14.1 [−54.5]*	*−24.7 [−62.5]*
25B	Ph, Ph	28.5 [8.6]	28.4 [8.1]	28.5 [12.3]
27B	Ph, Ph	*−21.9 [−41.8]*	*−21.7 [−42.1]*	*−32.6 [−48.8]*
25C	$SiMe_3$, Ph	22.8 [15.2]	23.0 [14.7]	22.1 [18.5]
27C	$SiMe_3$, Ph	*−31.9 [−24.9]*	*−31.6 [−24.5]*	*−43.3 [−46.9]*
25D	Ph, $SiMe_3$	27.6 [12.9]	27.7 [12.3]	27.1 [16.6]
27D	Ph, $SiMe_3$	*−52.5 [−24.9]*	*−52.2 [−24.5]*	*−63.5 [−46.9]*
25E	$SiMe_3$, $SiMe_3$	15.6 [17.4]	15.8 [16.6]	15.6 [22.7]
27E	$SiMe_3$, $SiMe_3$	*−39.6 [−37.9]*	*−39.4 [−38.6]*	*−49.9 [−42.8]*

[a] Reaction energies are italicized. Values in brackets are energetics compared to the iridium vinylcyclopropene species **20A**−**E** (kcal mol^{-1}). [b] Values are ZPE-corrected. [c] Corrections done at 298 K.

Computational analyses for iridabenzenes **24C** and **24D** reveal the barriers for C−C bond coupling are quite different. In agreement with the experimental results for **10** and **12**, transition structure **25C** has a barrier of 22.1 kcal mol^{-1}, while **25D** has a barrier of 27.1 kcal mol^{-1}. This is consistent with the C1 position being directly involved with the C−C bond coupling process and $SiMe_3$ group having in general a larger effect on the barrier than Ph. The largest geometric difference between **25B** and **25C**/**D** is the dihedral angle *D*(CB−C2−C3−C4), which is 160.6°, due to repulsion from the adjacent $SiMe_3$ group, compared to 180.0° for **25B**.

The lowest barrier for rearrangement was computed for bis(trimethylsilyl) **25E**. The $\Delta G^{\ddagger}$ value is only 15.6 kcal mol^{-1},

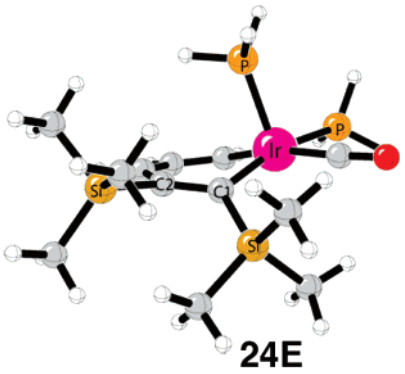

Figure 7. Nonplanar minimum for bis(trimethylsilyl) **24E**.

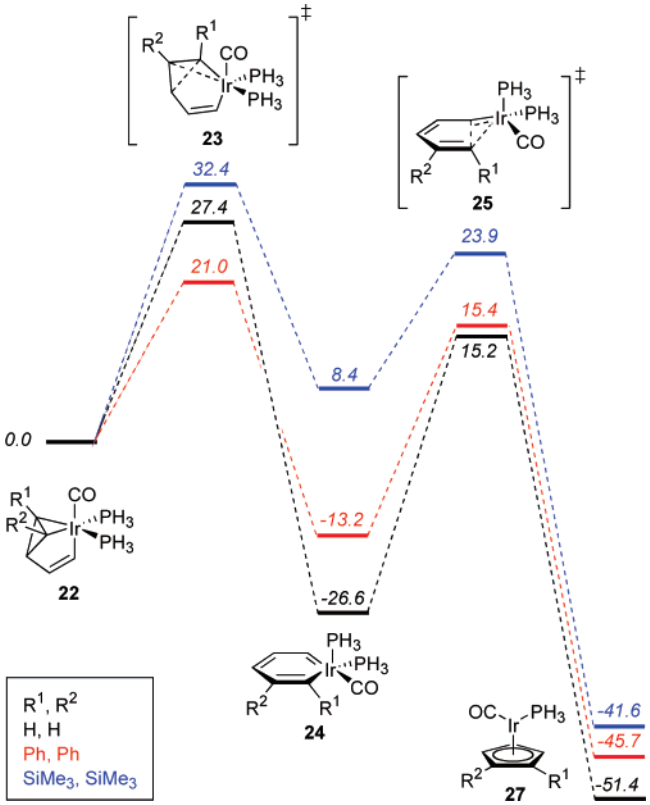

Figure 8. Free-energy potential surfaces (kcal mol^{-1}) for the rearrangements of **22A** (black), **22B** (red), and **22E** (blue).

indicating a very facile reaction (and thus why we never observe **16**). Similar to phenyl substitution, the barrier for **25E** is lower than expected on the basis of individual effects of *meta* or *ortho* $SiMe_3$ groups, since the ground state is destabilized due to adjacent bulky $SiMe_3$ groups. In fact, the repulsion is so large that the lowest energy geometry of **24E** is nonplanar (Figure 7).[27c] The $SiMe_3$ groups have a dihedral angle (Si−C1−C2−Si) of 36.9°, and the C2 carbon is slightly pyramidalized to 2.2°. This nonplanar structure for **24E** is 2.1 kcal mol^{-1} lower in energy than the planar geometry. Progression toward the transition state **25E** maximizes the relief of this repulsive interaction, with a dihedral angle *D*(Si−C1−C2−Si) of 81.4°. In the bis(trimethylsilyl) cyclopentadienyl complex **27E** this dihedral decreases to 4.4° to allow for anion delocalization.

Finally, Figure 8 depicts a composite of the potential energy surfaces for conversion of benvalenes **22A**, **22B**, and **22E** to their respective η^5-cyclopentadienyliridium complexes **27**. These potential energy surfaces clearly show the dramatic reactivity difference between trimethylsilyl and phenyl groups at R^1 and R^2. The largest difference in these surfaces is the (relatively) shallow minimum associated with iridabenzene **24E** on the blue surface (as discussed above).

Conclusions

The reaction of 1-phenyl-2-trimethylsilyl- or 1,2-bis(trimethylsilyl)-substituted 3-iodovinylcyclopropenes with Vaska's and Vaska-type complexes produced either iridabenzenes, iridabenzvalenes, and/or cyclopentadienyliridium complexes, depending on both the substituents on the C_5 framework and the phosphine ligands on the Ir center. Compared to previous results with the diphenylcyclopropene analogue, inclusion of $SiMe_3$ groups stabilizes the iridabenzvalene and correspondingly destabilizes the iridabenzene when utilizing PPh_3 ligands. Switching to more electron-rich phosphines afforded iridabenzvalenes that were stable for extended periods at 75 °C. Hybrid-DFT calculations along the minimum energy pathway for conversion of iridavinylcyclopropenes **20A**−**E** to cyclopentadienyliridium complexes **27A**−**E** revealed that phenyl- and trimethylsilyl-substituted benzvalenes form relatively weak π-complexes due to steric repulsions, and the barrier for rearrangement to iridabenzene is controlled by electronic effects in the transition state and not the degree of π-complexation. Trimethylsilyl-substituted benzvalenes have larger barriers for rearrangement than Ph-substituted species. For iridabenzvalene **9(22C/D)**, there is a preference for breakage of the Ir−C bond with the $SiMe_3$ attached due to charge stabilization. For the C−C bond coupling carbene migration of iridabenzene to the cyclopentadienyliridium complex, *ortho*-trimethylsilyl- and *ortho,meta*-bis(trimethylsilyl)iridabenzenes have low barriers for rearrangement, due to direct electronic effects at the *ortho* position. Also, the bis(trimethlysilyl)iridabenzene has significant steric repulsion between adjacent groups, leading to a nonplanar geometry, that is relieved in the transition state, making this a very facile rearrangement process. Future work will focus on the preparation of irida-aromatics with different substituents, as well as reaction of cyclopropene ligands **5a**,**b** with additional transition metal complexes. The results of these studies will be reported shortly.

Experimental Section

(Iodomethyl)triphenylphosphonium iodide,[17] 1,1,1-triacetoxy-1,1-dihydro-1,2-benziodoxol-3(1*H*)-one,[16] the Vaska-type complexes,[29] and cyclopropene derivatives **6b**−**8b**[15] were prepared according to literature procedures. All other chemicals were purchased from commercial suppliers and used as received. Column chromatography was performed on Whatman reagent grade silica gel (230−400 mesh). Manipulation of organometallic reagents was carried out using either a Vacuum Atmospheres inert atmosphere glovebox or standard Schlenk techniques. THF, Et_2O, and hexanes were distilled from Na/benzophenone and degassed by three freeze/pump/thaw cycles prior to use. Toluene and benzene were distilled from $LiAlH_4$ and degassed by three freeze/pump/thaw cycles prior to use. NMR spectra were recorded on a Varian Unity-INOVA 300 spectrometer at ambient temperature. ^{1}H, ^{13}C, and ^{31}P NMR spectra were acquired at 299.95, 75.43, and 121.42 MHz, respectively. Chemical shifts for ^{1}H and ^{13}C NMR spectra are reported in parts per million (δ) downfield from tetramethylsilane using the residual

(29) (a) Collman, J. P.; Sears, C. T., Jr.; Kubota, M. *Inorg. Synth.* **1973**, *14*, 92−93. (b) Burk, M. J.; Crabtree, R. H. *Inorg. Chem.* **1986**, *25*, 931−932.

solvent signal ($CDCl_3$: ^1H 7.26, ^{13}C 77.00; C_6D_6: ^1H 7.16, ^{13}C 128.39) as an internal standard. The ^{31}P NMR spectrum is referenced relative to external H_3PO_4 or PPh_3. Coupling constants are reported in hertz. FT-IR spectra were recorded using a Nicolet Magna 550 FT-IR spectrometer. Elemental analyses were performed by Robertson Microlit Laboratories, Inc.

Ethyl 2-phenyl-3-trimethylsilyl-2-cyclopropenecarboxylate (6a). A mixture of 1-phenyl-2-(trimethylsilyl)acetylene (60 g, 0.34 mol) and Cu powder (1.2 g, 0.02 mol) was heated to 130 °C under N_2. A solution of ethyl diazoacetate (14 g, 0.12 mol) and cyclohexane (15 mL) was added dropwise to the stirring suspension via syringe at a rate of 1 mL/h. After addition was complete, the mixture was heated an additional 1 h and then cooled. The excess 1-phenyl-2-(trimethylsilyl)acetylene was distilled under vacuum. The resulting residue was chromatographed to give **6a**[14] as a colorless oil (8.93 g, 30% based on ethyl diazoacetate). Spectroscopic data matched those previously reported.[14]

3-Hydroxymethyl-1-phenyl-2-trimethylsilyl-1-cyclopropene (7a). To a solution of **6a** (2.2 g, 8.45 mmol) in THF (40 mL) cooled to 0 °C was added DIBAL-H (12.67 mL, 1 M in hexane, 12.67 mmol) via syringe over 5 min. The solution was stirred at 0 °C until no starting material was visible by TLC. The mixture was transferred to a separatory funnel, and potassium sodium tartrate (Rochelle's salt, 2.75 g) and water (10 mL) were added. After shaking, the gel formed was extracted with Et_2O (3 × 25 mL). The combined organics were dried ($MgSO_4$) and the solvent removed *in vacuo*. Chromatography of the residue on silica (4:1 hexanes/Et_2O) afforded **7a** (1.52 g, 81%) as a colorless oil. ^1H NMR ($CDCl_3$): δ 7.44 (d, J = 8.4 Hz, 2H), 7.26 (t, J = 7.5 Hz, 2H), 7.24 (t, J = 7.8 Hz, 1H), 3.50 (t, J = 4.7 Hz, 2H), 1.83 (t, J = 4.7 Hz, 1H), 1.10 (br s, 1H), 0.15 (s, 9H). ^{13}C NMR ($CDCl_3$): δ 135.75, 130.33, 129.58, 129.27, 128.92, 115.63, 69.35, 21.99, −0.74. IR (Et_2O): ν 3333 (OH) cm^{-1}.

2-Phenyl-3-trimethylsilyl-2-cyclopropenecarbaldehyde (8a). A solution of **7a** (1.51 g, 6.87 mmol) in CH_2Cl_2 (20 mL) was added dropwise to a mixture of 1,1,1-triacetoxy-1,1-dihydro-1,2-benziodoxol-3(1*H*)-one (3.8 g, 9.36 mmol) and CH_2Cl_2 (40 mL), and the resulting mixture was stirred for 30 min at room temperature. The reaction was quenched with 1 N NaOH solution (70 mL) and the organic phase extracted with Et_2O (2 × 60 mL). The organic layer was dried ($MgSO_4$) and the solvent removed *in vacuo*. Chromatography of the residue on silica (6:1 hexanes/Et_2O) gave **8a** (1.05 g, 71%) as a colorless oil. ^1H NMR ($CDCl_3$): δ 8.77 (d, J = 7.8 Hz, 1H), 7.55 (d, J = 7.5 Hz, 2H), 7.47 (t, J = 7.2 Hz, 2H), 7.45 (t, J = 7.2 Hz, 1H), 2.56 (d, J = 7.5 Hz, 1H), 0.35 (s, 9H). ^{13}C NMR ($CDCl_3$): δ 205.62, 130.49, 130.20, 129.14, 127.98, 125.25, 109.08, 34.11, −1.29. IR (Et_2O): ν 1690 (s, C═O) cm^{-1}.

(*Z*)-3-(2-Iodoethenyl)-1-phenyl-2-(trimethylsilyl)-1-cyclopropene (5a). (Iodomethyl)triphenylphosphonium iodide (3.47 g, 6.54 mmol) was dried at 100 °C under vacuum for 30 min prior to use. The phosphonium salt was suspended in THF (15 mL) under an N_2 atmosphere, $NaN(SiMe_3)_2$ (1 M in THF, 5.95 mL, 5.95 mmol) was added via syringe, and the mixture was stirred for 5 min to give a yellow solution. The reaction was cooled to −78 °C, and HMPA (2.0 mL) was added and stirred for 10 min. Aldehyde **8a** (1.55 g, 7.17 mmol) in THF (5 mL) was then added, and the reaction was stirred until no **8a** was detected by TLC (ca. 30 min). The mixture was filtered through a short silica column and washed with Et_2O until no product was eluted further. The solvent was removed *in vacuo* and the residue chromatographed on silica gel (hexanes) to give **5a** (1.35 g, 58%) as a colorless oil. The material was stored at −30 °C, and a few crystals of hydroquinone were added to neat **5a** to inhibit decomposition. ^1H NMR ($CDCl_3$): δ 7.38 (d, J = 6.9 Hz, 2H), 7.27 (t, J = 7.2 Hz, 2H), 7.25 (t, J = 7.2 Hz, 1H), 5.78 (d, J = 7.5 Hz, 1H), 5.55 (t, J = 7.5 Hz, 1H), 2.42 (d, J = 7.5 Hz, 1H), 0.15 (s, 9H). ^{13}C NMR ($CDCl_3$): δ 146.96, 132.30, 129.64, 129.55, 129.51, 128.95, 114.8, 76.17, 26.93, −0.94. IR (Et_2O): ν 1847 (cyclopropene C═C) cm^{-1}.

(*Z*)-3-(2-Iodoethenyl)-1,2-bis(trimethylsilyl)-1-cyclopropene (5b). As described above for the preparation of compound **5a**, (iodomethyl)triphenylphosphonium iodide (1.23 g, 2.32 mmol) was treated with $NaN(SiMe_3)_2$ (1 M in THF, 2.1 mL, 2.1 mmol) and HMPA (0.7 mL), respectively. Wittig reaction of the resulting ylide with aldehyde **8b** (0.55 g, 2.58 mmol) gave **5b** (0.25 g, 35%) as a colorless oil after chromatography on silica (hexanes). The pure material was stored similarly to **5a**. ^1H NMR ($CDCl_3$): δ 5.75 (d, J = 7.4 Hz, 1H), 5.45 (t, J = 7.4 Hz, 1H), 2.05 (d, J = 7.5 Hz, 1H), 0.20 (s, 18H). ^{13}C NMR ($CDCl_3$): δ 149.15, 134.75, 72.58, 25.00, −1.32.

Synthesis of Complexes 9−11. A flame-dried Schlenk flask (50 mL) was charged with cyclopropene **5a** (0.30 g, 0.93 mmol) and Et_2O (20 mL) and cooled to −78 °C. To this was added BuLi (375 μL, 2.5 M in hexane, 0.93 mmol) at −78 °C over 5 min. After stirring for 15 min at −78 °C, the resulting mixture was transferred over 5 min by a canula to a −78 °C suspension of $(PPh_3)_2Ir(CO)Cl$ (0.60 g, 0.76 mmol) in Et_2O (5 mL). The mixture was continuously stirred at −78 °C for 30 min and then slowly warmed to room temperature over a 3 h period. The solvent was removed under vacuum, and the residue was chromatographed over silica gel (8:1 hexane/Et_2O) to give a 10:3:2 mixture of complexes **9**, **10**, and **11** (329 mg, 47% combined yield). Benzvalene **9** could be isolated in pure form by reacting a mixture in EtOAc (2 mL) with excess MeI for 30 min, then adding hexanes (10 mL) and filtering off the unwanted salts. Cyclopentadienyl complex **11** could be isolated by refluxing the mixture in benzene for 24 h.

Iridabenzvalene 9. ^1H NMR (C_6D_6): δ 7.63−7.55 (m, 6H), 7.40−7.31 (m, 8H), 7.04−6.82 (m, 21H), 6.71−6.63 (m, 1H, *H4*), 6.39−6.28 (m, 1H, *H5*), 3.08 (br s, 1H, *H3*), 0.05 (s, 9H, $Si(CH_3)_3$). ^{13}C NMR (C_6D_6): δ 181.58 (t, J = 6.0 Hz, CO), 151.24 (t, J = 14.1 Hz), 145.76 (br s), 144.15 (t, J = 7.1 Hz), 137.25 (dd, J = 40.3, 4.0 Hz), 135.58 (dd, J = 41.3, 10.7 Hz), 134.67 (d, J = 10.1 Hz), 134.18 (d, J = 10.1 Hz), 129.65 (s), 129.24 (s), 127.99 (d, J = 9.1 Hz), 124.27 (s), 75.81 (d, J = 58.4 Hz), 56.97 (s), 55.54 (d, J = 53.4 Hz), 0.40 (s). ^{31}P NMR (C_6D_6): δ 23.01 (s). IR (Et_2O): ν 1983 (s, CO) cm^{-1}. Anal. Calcd for $C_{51}H_{47}IrOP_2Si$: C, 63.93; H, 4.94. Found: C, 64.18; H, 5.35.

Iridabenzene 10. Partial ^1H NMR (C_6D_6): δ 10.45 (dt, J = 11.7, 11.4 Hz, 1H), 8.14 (dt, J = 7.3, 7.0 Hz, 1H). The remaining signals overlapped with the large quantities of **9** and **11**, which proved impossible to remove to any significant degree.

η^5-Cyclopentadienyliridium 11. ^1H NMR (C_6D_6): δ 7.80−7.65 (m, 8H), 7.08−6.91 (m, 12H), 5.40 (dd, J = 2.3, 1.8 Hz, 1H), 4.67 (dd, J = 2.3, 1.8 Hz, 1H), 4.54 (ddt, J = 2.6, 2.3, 0.9 Hz, 1H), 0.28 (s, 9H, $Si(CH_3)_3$). ^{13}C NMR (C_6D_6): δ 178.96 (d, J = 18.1, CO), 138.26 (s), 137.40 (d, J = 12.1 Hz), 134.69 (d, J = 12.1 Hz), 132.26 (s), 130.42 (d, J = 2.0 Hz), 128.47 (d, J = 2.0 Hz), 128.35 (s), 127.72 (s), 111.85 (d, J = 7.1 Hz), 92.25 (d, J = 4.0 Hz), 91.06 (s), 89.67 (s), 85.47 (s), 1.76 (s). ^{31}P NMR (C_6D_6): δ 17.97 (s). IR (Et_2O): ν 1936 (s, CO) cm^{-1}. Anal. Calcd for $C_{33}H_{32}IrOPSi$: C, 56.96; H, 4.63. Found: C, 56.80; H, 4.58.

Thermal Conversion of 9 to 11 via 12. Benzvalene **9** (100 mg, 0.104 mmol) was heated in C_6D_6 for 24 h at 75 °C. Chromatography over silica (6:1 hexane/Et_2O) gave complex **11** (62 mg, 89% yield) as bright yellow crystals. If the reaction was stopped after 10 h, chromatography of the mixture gave Cp complex **11** and a 3:2 mixture of **11** and **12**, the latter for spectral analysis.

Iridabenzene 12. ^1H NMR (C_6D_6): δ 10.85 (ddt, J = 11.7, 10.8, 1.2 Hz, 1H, *H5*), 8.78 (dt, J = 6.8, 6.2 Hz, 1H, *H3*), 7.65−7.26 (m, 15H), 7.12−6.87 (m, 21H), 0.28 (s, 9H, $Si(CH_3)_3$). ^{13}C NMR (C_6D_6): δ 188.93 (s), 188.00 (t, J = 6.0 Hz), 171.27 (t, J = 4.0 Hz), 145.32 (t, J = 8.0 Hz), 141.37 (dd, J = 16.1, 4.0 Hz),

137.15 (d, $J = 5.0$ Hz), 134.68 (s), 132.70 (s), 129.97 (s), 128.95 (s), 128.24 (s), 126.56 (s), 124.35 (s), 3.67 (s). ^{31}P NMR (C_6D_6): δ 17.13 (s).

Diiridium Complex 13. Reaction of cyclopropene **5a** (0.30 g, 0.93 mmol) with BuLi (2.5 M in hexane, 0.375 μL, 0.93 mmol) and then with $(Ph_3P)_2Ir(CO)Cl$ (0.60 g, 0.93 mmol) in Et_2O at −78 °C gave a mixture that was slowly warmed to room temperature over a 3 h period. Workup was as described above for the preparation of **9**−**11**. The crude residue was redissolved in benzene (2 mL) and heated for 24 h at 75 °C. Chromatography over silica (6:1 hexane/Et_2O) yielded complexes **11** (0.26 g, 39%) and **13** (0.02 g, 4%). Red crystals of **13** were obtained by recrystallization in Et_2O/hexane overnight at −30 °C. ^{1}H NMR (C_6D_6): δ 10.91 (d, $J = 8.8$ Hz, 1H), 7.92−7.80 (m, 7H), 7.66−7.55 (m, 6H), 7.18−7.10 (m, 6H), 7.09−6.99 (m, 9H), 6.98−6.83 (m, 5H), 6.12−6.02 (m, 1H), 5.86−5.76 (m, 1H), 5.20−5.12 (m, 1H), −0.07 (s, 9H). ^{13}C NMR (C_6D_6): 179.96 (d, $J = 7.6$ Hz, CO), 174.82 (d, $J = 15.1$ Hz, CO), 160.01 (s), 152.12 (s), 142.97-(dd, $J = 21.4$ Hz, 6.6 Hz), 136.90 (s), 136.12 (s), 135.69 (s), 135.29 (t, $J = 5.0$ Hz),134.83 (d, $J = 12.1$ Hz), 134.33 (d, $J = 10.1$ Hz), 130.61 (s), 125.89 (s), 130.03 (s), 128.52 (s), 127.80 (s), 126.21 (s), 125.89 (s), 125.00 (s), 109.69 (s), 98.65 (s), 95.72 (s), 2.05 (s). ^{31}P NMR (C_6D_6): δ 17.00 (d, $J = 8.5$ Hz), 11.06 (d, $J = 8.5$ Hz). IR (Et_2O): ν 2026, 1950 (s, CO) cm^{-1}. Anal. Calcd for $C_{52}H_{47}IIr_2O_2P_2Si$: C, 47.99; H, 3.33. Found: C, 47.75; H, 3.47.

Synthesis of Benzvalene 14. Cyclopropene **5b** (0.17 g, 0.5 mmol) was reacted with BuLi (2.5 M in hexanes, 0.22 mL, 0.55 mmol) and $(Ph_3P)_2Ir(CO)Cl$ (0.47 g, 0.6 mmol) as described above for the preparation of **9**. The mixture was filtered through silica and washed with small amounts of Et_2O. The filtrate was concentrated and hexane was added. The resulting solution was stored at −30 °C overnight to give **14** (0.39 g, 40%) as pale yellow crystals. ^{1}H NMR (C_6D_6): δ 7.61−7.55 (m, 10H), 7.08−6.90 (m, 20H), 6.51−6.44 (m, 1H, *H5*), 5.84 (ddt, $J = 8.2$, 7.9, 2.6 Hz, 1H, *H4*), 2.71−2.66 (m, 1H, *H3*), 0.22 (s, 18H, Si(CH_3)$_3$). ^{13}C NMR (C_6D_6): δ 180.92 (t, $J = 6.0$ Hz, CO), 152.92 (t, $J = 14.1$ Hz), 144.40 (t, $J = 9.1$ Hz), 137.25 (t, $J = 22.2$ Hz), 134.66 (dd, $J = 5.0$ Hz), 129.6 (s), 127.75 (t, $J = 5.0$ Hz), 62.70 (m), 54.22 (t, $J = 4.0$ Hz), 1.72 (s). ^{31}P NMR (C_6D_6): δ −3.09 (s). IR (Et_2O): ν 1973 (s, CO) cm^{-1}. Anal. Calcd for $C_{48}H_{51}IrOP_2Si_2$: C, 60.42; H, 5.39. Found: C, 60.22; H, 5.39.

Synthesis of η^5-Cyclopentadienyliridium 15. A solution of **14** (100 mg, 0.105 mmol) in benzene (5 mL) was heated at 75 °C for 24 h. The mixture was cooled and the solvent removed *in vacuo*. Chromatography of the residue on silica (6:1 hexane/Et_2O) gave complex **15** (67 mg, 93%) as yellow crystals. ^{1}H NMR (C_6D_6): δ 7.84−7.77 (m, 6H), 7.09−6.94 (m, 9H), 5.12 (d, $J = 4.3$ Hz, 2H), 4.73−4.70 (m, 1H), 0.44 (s, 18H, Si(CH_3)$_3$). ^{13}C NMR (C_6D_6): δ 178.24 (d, $J = 18.1$, CO), 137.69 (d, $J = 57.4$ Hz), 134.28 (d, $J = 12.1$ Hz), 129.95 (d, $J = 2.0$ Hz), 127.86 (s), 95.61 (s), 93.48 (s), 93.41 (s), 87.93 (s), 2.03 (s). ^{31}P NMR (C_6D_6): δ 17.84 (s). IR (Et_2O): ν 1940 (s, CO) cm^{-1}. Anal. Calcd for $C_{30}H_{36}IrOPSi_2$: C, 52.07; H, 5.24. Found: C, 51.91; H, 5.34.

General Preparation of Benzvalenes 17a−e. Reaction of cyclopropene **5a** with BuLi, then with $(R_3P)_2Ir(CO)Cl$ in Et_2O at −78 °C, gave a mixture that was slowly warmed to room temperature over a 3 h period. Workup was as described above for the preparation of **9**. The resulting mixture was treated with Bu_4NF (1 M in THF, 2 equiv) and stirred for 5 h. Filtration and removal of the volatiles *in vacuo* gave **17a**−**e** as pale yellow oils.

Iridabenzvalene 17a: 50% yield. ^{1}H NMR (C_6D_6): δ 7.60 (d, $J = 7.3$ Hz, 2H, *o-H* Ph), 7.22 (t, $J = 7.6$ Hz, 3H, *m-H* Ph), 7.04−6.94 (m, 2H, *p-H* Ph and *H4*), 6.45−6.36 (m, 1H, *H5*), 3.12 (br s, 1H, *H3*), 1.31 (d, $J = 8.8$ Hz, 9H), 1.08 (d, $J = 8.8$ Hz, 9H), 0.27 (s, 9H, Si(CH_3)$_3$). ^{13}C NMR (C_6D_6): δ 179.74 (t, $J = 7.0$ Hz, CO), 148.81 (br s), 146.62 (t, $J = 8.1$ Hz), 141.13 (t, $J = 15.1$ Hz), 128.18 (s), 127.56 (s), 127.53 (s), 123.97 (s), 74.97 (d, $J = 62.4$ Hz), 58.06 (d, $J = 54.4$ Hz), 55.46 (t, $J = 4.0$ Hz), 21.40 (dd, $J = 28.2$ Hz, $J = 4.0$ Hz), 19.87 (dd, $J = 29.2$ Hz, $J = 3.0$ Hz), 0.49 (s). ^{31}P NMR (C_6D_6): δ 29.24 (d, $J = 37.6$ Hz), 28.52 (d, $J = 37.6$ Hz). IR (Et_2O): 1971 cm^{-1}.

Iridabenzvalene 17b: 85% yield. ^{1}H NMR (C_6D_6): δ 7.60 (d, $J = 7.3$ Hz, 2H, *o-H* Ph), 7.31−6.97 (m, 14H), 6.60−6.48 (m, 1H, *H5*), 3.11−3.14 (br s, 1H, *H3*), 1.63 (d, $J = 7.91$ Hz, 3H), 1.46 (d, $J = 8.2$ Hz, 3H), 1.36 (d, $J = 8.2$ Hz, 3H), 1.19 (d, $J = 8.1$ Hz, 3H), 0.24 (s, 9H, Si(CH_3)$_3$). ^{13}C NMR (C_6D_6): δ 179.89 (t, $J = 7.0$ Hz, CO), 148.17 (br s), 146.27 (t, $J = 8.1$ Hz), 142.73 (t, $J = 15.1$ Hz), 141.61 (dd, $J = 35.2$ Hz, $J = 7.0$ Hz), 140.42 (dd, $J = 34.2$ Hz, $J = 6.0$ Hz), 129.59 (d, $J = 9.1$ Hz), 129.14 (d, $J = 9.1$ Hz), 128.93 (d, $J = 2.0$ Hz), 128.65 (d, $J = 2.0$ Hz), 128.30 (s), 127.56 (s), 128.15 (s), 127.66 (s, 2C), 124.18 (s), 73.98 (dd, $J = 54.4$ Hz, $J = 6.0$ Hz), 57.62 (dd, $J = 48.3$ Hz, $J = 3.0$ Hz), 55.97 (t, $J = 4.0$ Hz), 21.40 (dd, $J = 28.2$ Hz, $J = 7.0$ Hz), 19.04 (dd, $J = 30.2$ Hz, $J = 7.0$ Hz), 17.81 (dd, $J = 29.2$ Hz, $J = 7.0$ Hz), 15.38 (dd, $J = 28.2$ Hz, $J = 5.0$ Hz), 0.48 (s). ^{31}P NMR (C_6D_6): δ 41.13 (d, $J = 36.9$ Hz), 40.66 (d, $J = 36.9$ Hz). IR (Et_2O): 1980 cm^{-1}.

Iridabenzvalene 17c: 42% yield. ^{1}H NMR (C_6D_6): δ 7.66 (d, $J = 7.3$ Hz, 2H, *o-H* Ph), 7.23 (t, $J = 7.6$ Hz, 2H, *m-H* Ph), 7.02 (t, $J = 7.3$ Hz, 1H, *p-H* Ph), 6.88−6.81 (m, 1H, *H4*), 6.68−5.59 (m, 1H, *H5*), 3.09 (br s, 1H, *H3*), 1.84−1.38 (m, 12H), 0.98−0.84 (m, 9H), 0.78−0.66 (m, 9H), 0.30 (s, 9H, Si(CH_3)$_3$). ^{13}C NMR (C_6D_6) δ 180.68 (t, $J = 7.5$ Hz, CO), 149.25 (dd, $J = 6.0$, 4.0 Hz), 145.69 (t, $J = 7.1$ Hz), 139.92 (t, $J = 15.1$ Hz), 127.82 (s), 127.79 (s), 124.10 (s), 72.11 (dd, $J = 62.4$, 4.0 Hz), 55.46 (t, $J = 3.0$ Hz), 54.72 (dd, $J = 57.4$, 4.5 Hz), 21.72 (d, $J = 26.2$ Hz), 20.46 (d, $J = 25.2$ Hz), 8.20 (s), 7.52 (s), 0.47 (s). ^{31}P NMR (C_6D_6): δ −19.30 (d, $J = 37.1$ Hz), 21.32 (d, $J = 37.1$ Hz). IR (Et_2O): 1966 cm^{-1}.

Iridabenzvalene 17d: 59% yield. ^{1}H NMR (C_6D_6): δ 7.57−7.48 (m, 5H), 7.33−7.23 (m, 4H), 7.18−6.86 (m, 17H), 6.83−6.73 (m, 1H), 3.46 (br s, 1H), 1.73 (d, $J = 7.8$ Hz, 3H,), 1.55 (d, $J = 8.2$ Hz, 3H,), 0.20 (s, 9H, Si(CH_3)$_3$). ^{13}C NMR (C_6D_6): δ 180.19 (t, $J = 6.0$ Hz, CO), 147.37 (dd, $J = 6.0$, 3.0 Hz), 145.87 (t, $J = 8.0$ Hz), 144.69 (t, $J = 14.5$ Hz), 138.58 (m, 2C), 133.15 (d, $J = 11.1$ Hz), 132.55 (d, $J = 10.1$ Hz), 132.18 (d, $J = 12.1$ Hz), 131.96 (d, $J = 10.8$ Hz), 129.45 (dd, $J = 28.2$, 2.0 Hz), 129.39 (d, $J = 17.1$ Hz), 128.20 (s), 128.00 (s), 127.83 (s), 124.15 (s), 76.90 (dd, $J = 65.5$ Hz, $J = 3.0$ Hz), 58.79 (dd, $J = 57.4$, 4.0 Hz), 56.91 (t, $J = 4.0$ Hz), 18.54 (d, $J = 31.2$ Hz), 16.87 (d, $J = 33.2$ Hz), 0.84 (s). ^{31}P NMR (C_6D_6): δ −23.27 (d, $J = 39.7$ Hz), −24.76 (d, $J = 39.7$ Hz). IR (Et_2O): 1986 cm^{-1}.

Iridabenzvalene 17e: 63% yield. ^{1}H NMR (C_6D_6): δ 7.68 (d, $J = 7.3$ Hz, 2H), 7.23 (d, $J = 7.5$ Hz, 2H), 7.04 (t, $J = 7.5$ Hz, 1H), 6.92−6.78 (m, 2H), 3.12 (br s, 1H), 2.22−1.93 (m, 12H), 1.80−1.72 (m, 6H), 1.18−0.88 (m, 36H), 0.34 (s, 9H, Si(CH_3)$_3$). ^{13}C NMR (C_6D_6): δ 181.52 (t, $J = 6.5$ Hz, CO), 148.97 (dd, $J = 6.6$, 4.6 Hz), 145.81 (t, $J = 8.1$ Hz), 141.01 (t, $J = 15.1$ Hz), 127.91 (m, 2C), 124.06 (s), 72.79 (d, $J = 63.5$ Hz), 55.93 (br s), 54.81 (dd, $J = 59.4$, 3.8 Hz), 40.90 (d, $J = 21.1$ Hz), 39.91 (d, $J = 21.1$ Hz), 25.80 (d, $J = 7.0$ Hz), 25.63 (s), 0.68 (s). ^{31}P NMR (C_6D_6): δ 17.84 (d, $J = 35.1$ Hz), 18.78 (d, $J = 35.1$ Hz). IR (Et_2O): 1965 cm^{-1}.

Thermolysis of Benzvalene 17a. Complex **17a** (20 mg, 0.034 mmol) was dissolved in benzene-d_6 (0.5 mL) and heated at 75 °C for 24 h. ^{1}H NMR spectroscopy showed no changed. Switching to toluene-d_8 and heating at 100 °C for 24 h afforded a ~40:1 mixture of **17a** and **18a**, along with significant decomposition. Partial data for **18a**: ^{1}H NMR (C_7D_8) δ 11.08 (ddt, $J = 12.7$, 10.0, 1.2 Hz, *H5*), 8.52 (ddt, $J = 8.1$, 5.9, 1.2 Hz, *H3*), 7.70 (t, $J = 8.9$ Hz, *H4*).

Thermolysis of Benzvalene 17b. Complex **17b** (20 mg, 0.028 mmol) was dissolved in benzene-d_6 (0.5 mL) and heated at 75 °C for 24 h. ^{1}H NMR spectroscopy showed the solution to be a 20:1

mixture of **17b** and **18b**. Partial data for **18b**: ^{1}H NMR (C_6D_6) δ 11.28 (q, J = 11.3 Hz, *H*5), 8.72 (q, J = 8.5 Hz, *H*3), 7.91 (t, J = 8.6 Hz, *H*4).

Thermolysis of Benzvalene 17c. Complex **17c** (20 mg, 0.03 mmol) was dissolved in benzene-d_6 (0.5 mL) and heated at 75 °C for 24 h. ^{1}H NMR spectroscopy showed no change.

Thermolysis of Benzvalene 17d. Complex **17d** (20 mg, 0.024 mmol) was dissolved in benzene-d_6 (0.5 mL) and heated at 75 °C for 24 h. ^{1}H NMR spectroscopy showed the solution to be a 10:4:3 mixture of **17d**, **18d**, and **19d**, along with partial decomposition. Partial characterization data for **18d**: ^{1}H NMR (C_6D_6) δ 11.18 (q, J = 10.5 Hz, *H*5), 8.91 (q, J = 6.6 Hz, *H*3), 8.05 (t, J = 8.8 Hz, *H*4), 1.53 (d, J = 13.2 Hz), 0.34 (s).

The solution was heated further at 75 °C until NMR showed no remaining **17d** or **18d** (total time: 90 h). The solvent was removed and the residue was purified by chromatography on silica (6:1 hexane/Et_2O) to give **19d** (8.4 mg, 55%) as yellow crystals. ^{1}H NMR (C_6D_6): δ 7.72−7.67 (m, 2H), 7.65−7.53 (m, 4H), 7.13−7.00 (m, 9H), 5.41−5.37 (m, 1H), 4.79−4.75 (m, 1H), 4.62−4.58 (m, 1H), 2.03 (d, J = 9.7 Hz, 3H), 0.29 (s, 9H, Si(C*H*$_3$)$_3$). ^{13}C NMR (C_6D_6): δ 179.11 (d, J = 18.2 Hz, CO), 139.57 (m), 136.94 (s), 132.79 (s), 132.63 (s), 132.47 (s), 132.31 (s), 132.03 (s), 129.80 (m), 128.11 (s), 127.27 (s), 111.66 (s), 91.88 (s), 89.62 (s), 89.32 (s), 84.01(s), 21.52 (d, J = 42.3 Hz), 1.38 (s). ^{31}P NMR (C_6D_6): δ −4.85 (s). IR (Et_2O): ν 1937 (s, CO) cm^{-1}. Anal. Calcd for $C_{28}H_{30}$IrOPSi: C, 53.06; H, 4.77. Found: C, 53.22; H, 4.89.

Thermolysis of Benzvalene 17e. Complex **17e** (20 mg, 0.024 mmol) was dissolved in benzene-d_6 (0.5 mL) and heated at 75 °C for 24 h. The solvent was removed, and the residue was purified by chromatography on silica (6:1 hexane/Et_2O) to give **19e** (7.0 mg, 46%) as yellow crystals. ^{1}H NMR (C_6D_6): δ 7.69−7.74 (m, 2H), 7.02−7.21 (m, 3H), 5.46 (br s, 1H), 5.11 (br s, 1H), 4.83 (br s, 1H), 2.05−2.25 (m, 6H), 1.62−1.68 (m, 3H), 0.98−1.10 (m, 18H), 0.32 (s, 9H, Si(C*H*$_3$)$_3$). ^{13}C NMR (C_6D_6): δ 179.43 (d, J = 17.1 Hz, CO), 137.19 (s), 131.97 (s), 128.05 (s), 127.10 (s), 111.51 (d, J = 6.2 Hz), 91.52 (s), 88.27 (s), 86.47 (s), 82.37 (s), 40.48 (d, J = 33.2 Hz), 26.20 (s), 25.16 (s), 1.29 (s). ^{31}P NMR (C_6D_6): δ −3.61 (s). IR (Et_2O): ν 1937 (s, CO) cm^{-1}. Anal. Calcd for $C_{27}H_{44}$IrOPSi: C, 51.00; H, 6.97. Found: C, 50.82; H, 6.78.

X-ray Structure Determinations. Data were collected on an Enraf-Nonius CAD-4 Turbo diffractometer using Mo Kα radiation (λ = 0.71073 Å), graphite monochromator, T = 296 K, and scan mode $\omega-2\theta$. Pertinent crystallographic data and refinement parameters are given below. Structure refinement (C atoms anisotropic, H atoms riding) was accomplished with the teXsan program suite (version 1.7 for SGI workstations). The X-ray structures have been deposited with the Cambridge Crystallographic Data Centre as supplementary publication nos. CCDC-219153 (**13**) and CCDC-219154 (**14**). Copies of the data can be obtained free of charge on application to CCDC, 12 Union Road, Cambridge CB21EZ, UK (fax: (+44) 1223-336-033; e-mail: deposit@ccdc.cam.ac.uk).

Crystal structure of 13: $C_{52}H_{47}IIr_2O_2P_2Si\cdot 2CH_2Cl_2$, M_r = 1475.2, red block, 0.10 × 0.18 × 0.20 mm, monoclinic, space group $P2_1/a$, a = 18.558(3) Å, b = 15.874(3) Å, c = 20.342(2) Å, β = 112.65(2)°, V = 5530(2) Å^3, Z = 4, ρ_{calc} = 1.772 g cm^{-3}, μ = 56.9 cm^{-1}, $F(000)$ = 2840, $2\theta_{max}$ = 44°, 6327 independent reflections scanned, 4573 reflections in refinement [$I \geq \sigma(I)$], 541 parameters, R = 0.046, R_w = 0.049.

Crystal structure of 14. $C_{48}H_{51}IrOP_2Si_2$, M_r = 954.3, pale yellow prisms, 0.12 × 0.14 × 0.27 mm, triclinic, space group $P\bar{1}$, a = 11.958(3) Å, b = 13.111(2) Å, c = 14.535(4) Å, α = 95.28(3)°, β = 112.65(2)°, γ = 95.25(2)°, V = 2199.5(10) Å^3, Z = 2, ρ_{calc} = 1.441 g cm^{-3}, μ = 32.05 cm^{-1}, $F(000)$ = 964, $2\theta_{max}$ = 50°, 7812 independent reflections scanned, 7024 reflections in refinement [$I \geq \sigma(I)$], 488 parameters, R = 0.033, R_w = 0.038.

Acknowledgment. We thank the National Science Foundation (CHE-0075246 and -0647252) and the Schweizerischer Nationalfonds for support of this research. D.H.E. acknowledges the NSF IGERT program for a fellowship (DGE-0114443).

Supporting Information Available: X-ray structure cif files for compounds **13** and **14**; Cartesian coordinates and absolute electronic energies for structures **21**−**25** and **27**. This material is available free of charge via the Internet at http://pubs.acs.org.

OM700336D